Developmental Biology 377 (2013) 245–261

Contents lists available at SciVerse ScienceDirect

Developmental Biology

journal homepage: www.elsevier.com/locate/developmentalbiology

Evolution of Developmental Control Mechanisms

Canonical terminal patterning is an evolutionary novelty

Elizabeth J. Duncan, Matthew A. Benton [1], Peter K. Dearden *

Laboratory for Evolution and Development, Genetics Otago, Gravida; National Centre for Growth and Development, Department of Biochemistry, University of Otago, P.O. Box 56, Dunedin, Aotearoa, New Zealand

ARTICLE INFO

Article history:
Received 21 December 2012
Received in revised form
8 February 2013
Accepted 14 February 2013
Available online 22 February 2013

Keywords:
Terminal-patterning
Evolution
Development
Torso-like

ABSTRACT

Patterning of the terminal regions of the *Drosophila* embryo is achieved by an exquisitely regulated signal that passes between the follicle cells of the ovary, and the developing embryo. This pathway, however, is missing or modified in other insects. Here we trace the evolution of this pathway by examining the origins and expression of its components. The three core components of this pathway: trunk, torso and torso-like have different evolutionary histories and have been assembled step-wise to form the canonical terminal patterning pathway of *Drosophila* and *Tribolium*. Trunk, torso and a gene unrelated to terminal patterning, prothoraciotrophic hormone (PTTH), show an intimately linked evolutionary history, with every holometabolous insect, except the honeybee, possessing both *PTTH* and *torso* genes. Trunk is more restricted in its phylogenetic distribution, present only in the Diptera and *Tribolium* and, surprisingly, in the chelicerate *Ixodes scapularis*, raising the possibility that trunk and torso evolved earlier than previously thought. In *Drosophila* torso-like restricts the activation of the terminal patterning pathway to the poles of the embryo. Torso-like evolved in the pan-crustacean lineage, but based on expression of components of the canonical terminal patterning system in the hemimetabolous insect *Acyrthosiphon pisum* and the holometabolous insect *Apis mellifera*, we find that the canonical terminal-patterning system is not active in these insects. We therefore propose that the ancestral function of *torso-like* is unrelated to terminal patterning and that torso-like has become co-opted into terminal patterning in the lineage leading to Coleoptera and Diptera. We also show that this co-option has not resulted in changes to the molecular function of this protein. Torso-like from the pea aphid, honeybee and *Drosophila*, despite being expressed in different patterns, are functionally equivalent. We propose that co-option of torso-like into restricting the activity of trunk and torso facilitated the final step in the evolution of this pathway; the capture of transcriptional control of target genes such as *tailless* and *huckebein* by this complex and novel patterning pathway.

Introduction

In *Drosophila*, one of the earliest embryonic patterning events controls the specification of the anterior and posterior termini, via a process known as terminal-patterning. This process is controlled by maternal RNAs which are provided to the oocyte during oogenesis, and results in the spatially restricted activation of the receptor tyrosine kinase torso (tor) (Sprenger et al., 1989), by the presumptive ligand trunk (trk) (Casali and Casanova, 2001; Casanova, 1990; Casanova et al., 1995). The spatial restriction of this pathway to the poles of the embryo appears to be mediated by a third protein, torso-like (tsl) (Savant-Bhonsale and Montell, 1993), but the exact role of tsl in mediating this specificity is currently unknown (reviewed in Furriols and Casanova, 2003). Activation of tor causes an intracellular Ras-Raf-MAP-K/Erk phosphorylation cascade that ultimately leads to the expression of the zygotic target genes *tailless* (*tll*) and *huckebein* (*hkb*), likely via degradation of the transcriptional repressor capicua (Grimm et al., 2012). Correct expression of *tll* and *hkb* are integral for the specification of the non-segmented head and tail regions in *Drosophila*, the acron and the telson (Furriols and Casanova, 2003).

Components of this pathway, namely *tor* and *tsl*, are also required for patterning the anterior-most structure, the extraembryonic serosa, in *Tribolium castaneum* (Schoppmeier and Schroder, 2005). Recently, the *Tribolium* ortholog of *trk* has been shown to be maternally provided and essential for terminal pattering (Grillo et al., 2012). *Tribolium* is a short-germ band insect, in which the embryo extends from the posterior growth zone, which is segmented progressively, unlike *Drosophila*, a long-germ band insect, in which all segments are specified simultaneously (Davis and Patel, 2002). The terminal-patterning pathway

* Corresponding author. Fax: +64 3 479 7866.
E-mail addresses: elizabeth.duncan@otago.ac.nz (E.J. Duncan), mab97@cam.ac.uk (M.A. Benton), peter.dearden@otago.ac.nz (P.K. Dearden).
[1] Current address: Laboratory for Evolution and Development, Zoology Department, University of Cambridge, CB2 3EJ Cambridge, UK.

0012-1606/$ - see front matter © 2013 Elsevier Inc. All rights reserved.
http://dx.doi.org/10.1016/j.ydbio.2013.02.010

in *Tribolium* is required for setting up, or maintaining, the posterior growth zone, a process that requires *wingless* (*wg*) expression (Schoppmeier and Schroder, 2005; Schroder et al., 2000). The terminal-patterning pathway is also likely to be active in Diptera other than *Drosophila*, including the mosquito *Anopheles gambiae* (Goltsev et al., 2004) and the cyclorrhaphan fly *Episyrphus* (Lemke et al., 2010). The targets of the terminal patterning pathway are evolutionarily labile amongst the Diptera, for example *hkb* is not expressed in the blastoderm embryo of *Clogmia albipunctata* (Garcia-Solache et al., 2010) and in the cyclorrhaphan fly *Episyrphus* tor has additional roles in regulating anterior patterning, possibly through repression of *caudal* and activation of *orthodenticle* (Lemke et al., 2010).

The deeper evolutionary history of the canonical terminal-patterning pathway is, however, unclear, as key components of the pathway are missing in some insects, including the pea aphid (*Acyrthosiphon pisum*) (Shigenobu et al., 2010), the silkmoth (*Bombyx mori*) and the honeybee (*Apis mellifera*) (Dearden et al., 2006). Furthermore, canonical terminal patterning is not active in the long-germ band honeybee (Wilson and Dearden, 2009) or the jewel wasp *Nasonia vitripennis* (Lynch et al., 2012) and is not required to establish the early expression domains of the *tll* gene (Lynch et al., 2006; Wilson and Dearden, 2009).

Current phylogenomic studies place Hymenoptera as a basal radiation of the holometabolous insects (Krauss et al., 2008; Savard et al., 2006; Zdobnov and Bork, 2007) raising the question of whether terminal patterning is an ancestral trait in insects that has been lost selectively in the lineage leading to honeybees, or conversely, whether terminal patterning has evolved in the lineage leading to *Drosophila* and *Tribolium* (Lynch et al., 2012). To attempt to better understand the evolution of the canonical terminal patterning system, we have examined the evolution of its components using the genome sequences of diverse arthropods, and by examining expression of these genes in the holometabolous insect *A. mellifera*, and the hemimetabolous insect *A. pisum*.

Materials and methods

Insect culture

A. mellifera were cultured using standard techniques in Dunedin, New Zealand. *A. mellifera* embryos were collected from frames removed from nucleus boxes containing small *A. mellifera* colonies. *A. mellifera* queens were collected and dissected as previously described (Dearden et al., 2010). *Drosophila* were reared using standard techniques. The *A. pisum* strain used in this study was provided by Plant and Food Research, New Zealand. Parthenogenetic aphid clones were maintained on broad beans (*Vicia faba*) in growth chambers with a long-day photoperiod (16L:8D) at 15–20 °C. The sexual phenotype was induced transferring aphids to a growth chamber at 15 °C with short-day photoperiod (13L:11D). Aphid embryos were staged according to Miura et al. (2003) and Chang et al. (2006) Honeybee embryos were staged according to the scheme of DuPraw (1967) and stages of oogenesis according to Wilson et al. (2011). *Drosophila* embryos were staged according to the scheme of Campos-Ortega and Hartenstein (1997).

Phylogenetic and bioinformatics analyses

Orthologs of terminal patterning genes were obtained using a combination of methods; orthologs of *torso-like* were identified from genome data (Supplementary Table 1) using Blast algorithms (Altschul et al., 1990). Orthologs of *trk* and *PTTH* were identified by constructing a custom hidden Markov model (HMM) motif (Supplementary File 1), and using this motif to scan predicted protein sequences from databases (Supplementary Table 1) using the HMMER (v3.0) suite of programs (Eddy, 1998). HMM motifs are statistical models that define sequence similarity within a homologous gene family. These motifs can be used to scan protein sequences to identify potentially homologous proteins, even when the overall sequence conservation levels are quite low. Receptor tyrosine kinase domain containing proteins were also identified using HMMER and the pfam motif (PF07714.9).

Multiple alignments were carried out using ClustalX (Thompson et al., 1994) or Clustal Omega (Sievers et al., 2011) and analyzed using MrBAYES v3.1.2 (Ronquist and Huelsenbeck, 2003), initially under mixed models then using the most appropriate models (tsl phylogeny=Jones (Jones et al., 1992), trk/PTTH and tor phylogenies=WAG (Whelan and Goldman, 2001)). The Monte Carlo Markov Chain search was run with four chains over 1,000,000 generations with trees sampled every 1000 generations. The first 25% trees were discarded as 'burn-in'. Receptor tyrosine kinase domains extracted using HMMER (Eddy, 1998) were aligned using Clustal Omega (Sievers et al., 2011) and a neighbor-joining phylogeny was constructed using QuickTree v.1.1 (Howe et al., 2002) with 100 bootstrap replicates. The torso clade was then reanalyzed using Bayesian phylogeny, as detailed above.

In situ hybridization, immunohistochemistry, cuticle preparations and microscopy

In situ hybridization was carried out as previously described for honeybees (Dearden et al., 2010; Osborne and Dearden, 2005), aphids (Duncan and Dearden, 2010; Shigenobu et al., 2010) and *Drosophila* (Tautz and Pfeifle, 1989). Digoxigenin (DIG) labeled RNA probes were produced by *in vitro* transcription (refer to Supplementary Table 2 for primer sequences). All *in situ* hybridizations were carried out on at least three independent occasions and representative images are shown. Sense controls for these *in situ* hybridizations are provided in Supplementary Fig. 1.

Immunohistochemistry was carried out as previously described for aphids (Miura et al., 2003) with minor modifications; dissected ovaries were fixed for 30 min in a 1:1 mix of 4% formaldehyde:-heptane in PBS. After fixing, the lower (heptane) phase was removed and replaced with methanol equilibrated to −20 °C. Embryos were stored overnight in methanol at −20 °C before rehydration through a methanol:0.3% Triton-X 100 in 1 × PBS series. Following bleaching of endogenous peroxidases an antigen retrieval step was performed by incubating the ovaries at 95 °C in 0.01 M sodium citrate (pH 6.0) for 1 h. Activated ERK/MAPK was detected using a monoclonal antibody raised against the activated di-phosphorylated form of ERK (dp-ERK) (Sigma M8159) at a dilution of 1 in 100.

Drosophila immunohistochemistry was performed using anti-even-skipped (1 in 50; (Patel et al., 1994) or anti-dp-ERK (1:50; Sigma M8159). Secondary antibodies were diluted 1 in 200 and detected by 3,3-diaminobenzidine tetrahydrochloride (DAB) staining (Patel, 1994).

Cuticle preparations were prepared by mounting dechorionated *Drosophila* embryos in Hoyer's medium using established methods (Stern and Sucena, 2000) and visualized using darkfield microscopy.

Generation of transgenic Drosophila

Full-length coding sequences from *Drosophila*, honeybee and aphid *tsl* and aphid *tslr* were obtained by PCR and cloned into the Gateway entry vector PCR8 (Invitrogen). The sequence verified entry vector was then recombined into pP{UASp-DEST} (pPW) (Rorth, 1998), and germline transformants of *Drosophila* obtained by microinjection of the resulting plasmid into *Drosophila* w^{118} embryos (Rubin and Spradling, 1982). Expression was driven in the adult ovary by crossing *tsl* lines with the P[GawB]109C1 and

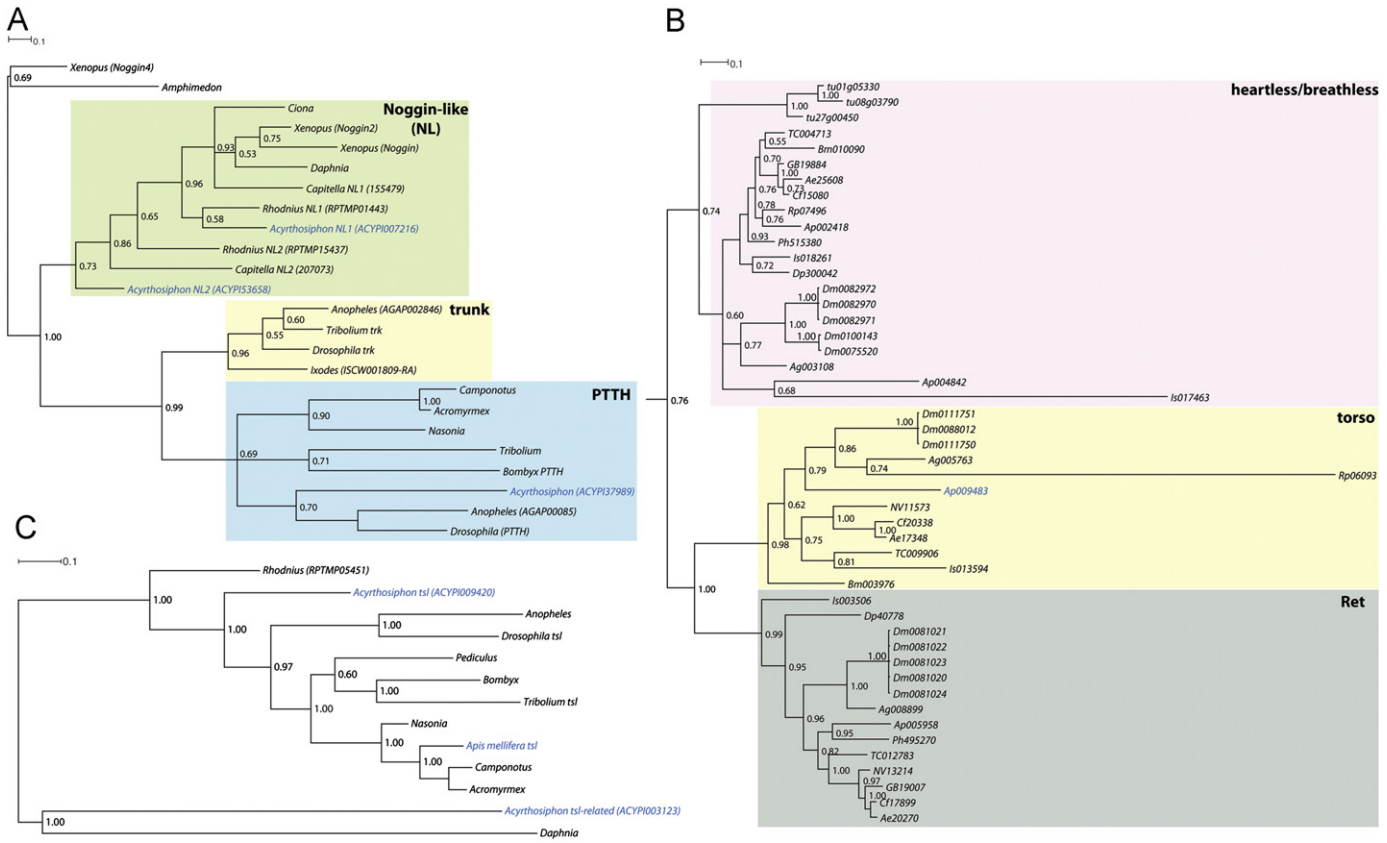

Fig. 1. Phylogeny of components of the canonical terminal-patterning pathway: (A) Bayesian phylogeny of arthropod Noggin-like proteins. Noggin-like domains were isolated from annotated protein sequences from sequenced metazoan genomes. Posterior probabilities are shown at nodes, tree is rooted with the Noggin-like sequence identified in the *Amphimedon* genome. This analysis reveals three well supported clades, an ancestral clade one corresponding to the "Noggin-like" proteins (green box). This clade contains representatives from the Lophotrochozoa, Deuterostomes and Ecdysozoa. The second clade contains the trunk proteins from *Drosophila* and *Tribolium* and the third clade the PTTH proteins. (B) Bayesian phylogeny of arthropod RTK sequences related to torso. Posterior probabilities are shown at nodes, tree is mid-point rooted. Three clades are identified, each clade, including the torso clade, contains at least one representative from the chelicerate *Ixodes* indicating that these RTK families were present in the last common ancestor of insects and chelicerates. Abbreviations are Ae=*Acromyrmex echinatior*, Ag=*Anopheles gambiae*, Ap=*Acyrthosiphon pisum*, Bm=*Bombyx mori*, Cf=*Camponotus floridanus*, Dp=*Daphnia pulex*, Dm=*Drosophila melanogaster*, Is=*Ixodes scapularis*, Nv=*Nasonia vitripennis*, Ph=*Pediculus humanus*, Rp=*Rhodnius prolixus*, Tc=*Tribolium castaneum*, tu=*Tetranychus urticae*. The numerical suffix refers to accession numbers from the relevant databases. (C) Bayesian phylogeny of torso-like protein sequences. Posterior probabilities are shown at nodes, tree is rooted with the crustacean *Daphnia pulex* torso-like protein. Nodes that are in blue font represent genes that were investigated by *in situ* hybridization in this study.

P[GawB]c135 GAL4 driver lines (data not shown) and with the the P[matalpha4-GAL-VP16]V37 driver line. *Drosophila* were maintained at 25 °C and crosses were set up and embryos collected on at least three independent occasions.

Results

Components of the terminal-patterning pathway arose independently at different points in the evolution of arthropods

Using available genome sequences (Supplementary Table 1), we attempted to identify orthologs of *trk*, *tor* and *tsl* in a number of diverse species. In order to sample the broadest phylogenetic range possible we selected taxa from the holometabolous insects (Diptera, Coleoptera, Lepidoptera and Hymenoptera), hemimetabolous insects (Hemiptera and Phthiraptera), crustacea (*Daphnia pulex*) and chelicerates *Ixodes scapularis* and *Tetranychus urticae*. For identifying sequences related to trk we extended this analysis beyond the Ecdysozoa, analyzing all of the genomes listed above, but also selecting representatives from the other two major groupings of animals; the Lophotrochozoans (*Capitella teleta*) and the Deuterostomes (*Xenopus tropicalis* and *Ciona intestinalis*). We also analyzed the genome of the basal metazoan *Amphimedon queenslandica*.

Trk, the ligand of the terminal patterning pathway in *Drosophila*, is a cysteine knot containing protein with weak similarity to the vertebrate Noggin family (Mushegian and Koonin, 1996). Using the Noggin HMM motif (PF05806.3) (Eddy, 1998) two proteins were identified in the *Drosophila* genome; Dm-trk and Dm-PTTH (prothoraciotrophic hormone). Which is expected as trk has been previously identified as the closest paralog of PTTH in holometabolous insects (Grillo et al., 2012; Rewitz et al., 2009). However, this HMM motif had limited power to detect orthologs of these genes in other insect species. A custom HMM motif was built using known trk and PTTH sequences from *Tribolium*, *Bombyx* and *Drosophila* (Supplementary File 1). This motif was used to screen all of the predicted proteins from the available arthropod genomes. This motif was also used to screen non-arthropod genomes including the Lophotrochozoan *C. teleta*, the Deuterostomes *X. tropicalis* and *C. intestinalis* and the basal metazoan *A. queenslandica*. Using this approach we recovered a number of protein sequences related to vertebrate Noggin proteins, we designated these as Noggin-like (NL) proteins.

Bayesian phylogenetic analysis of Noggin-like protein sequences robustly separates the resulting proteins into three clades (Fig. 1A), the NL clade containing the *Xenopus* Noggin proteins, a clade containing Dm-trk and a clade containing Dm-PTTH. This implies that PTTH and trk arose as a result of duplication and

divergence of an ancestral NL gene. Consistent with this hypothesis, we identify a non-trk/PTTH NL ortholog in the non-insect arthropod *D. pulex*, and two paralogs in the pea aphid (*Ap-NL1* and *Ap-NL2*). We cannot identify any NL genes in any currently sequenced holometabolous insects.

Orthologs of PTTH are found in all holometabolous insects species examined, with the exception of the honeybee. Of the three hemimetabolous insects included in this analysis only the pea aphid has an ortholog of PTTH, but both the pea aphid and *Rhodnius* have paralogs of NL genes. In contrast, orthologs of trk are only detected in *Drosophila*, *Tribolium* and the mosquito *A. gambiae*, all species which are known to have an active terminal-patterning pathway (Goltsev et al., 2004; Grillo et al., 2012; Schoppmeier and Schroder, 2005; Schroder et al., 2000). The trk-like clade also contains a protein sequence from the chelicerate *Ixodes*. This phylogeny implicates two alternative scenarios for the evolution of trk and PTTH. In the first, PTTH arose as a result of divergence and subsequent duplication of a *NL* gene in the insect lineage, and trk arose as a result of a subsequent round of duplication and divergence in the lineage leading to the Diptera and Coleoptera. The fact that a trk gene cannot be found in the Lepidopteran *Bombyx* implies a species-specific loss or may reflect gaps in the genome assembly. In this scenario, the grouping of the *Ixodes* protein with the insect trk proteins is a result of convergent evolution. In the second scenario, trk evolved deeper in the arthropod lineage, and has been duplicated to generate PTTH. This scenario implies at least five independent losses of trk in the evolution of arthropods. Analysis of protein sequence alignments reveals a domain of homology shared between the NL and trk proteins (Supplementary Fig. 2), that is not present in PTTH. This provides support for PTTH being the derived member of this protein family.

To identify possible orthologs of the receptor *tor*, all receptor tyrosine kinase (RTK) domain sequences were extracted from the predicted proteins of the fully sequenced genomes of *Drosophila melanogaster*, *A. gambiae*, *Bombyx mori*, *Tribolium castaneum*, *N. vitripennis*, *A. mellifera*, *Camponotus floridanus*, *Acromyrmex echinatior*, *A. pisum*, *Pediculus humanus*, *Rhodnius prolixus*, *T. urticae* and *I. scapularis*. Neighbor joining analysis (Supplementary File 2), revealed a cluster of putative torso receptor tyrosine kinases, grouping with the heartless/breathless and Ret receptor tyrosine kinase families. Bayesian phylogeny of these related families reveal the torso clade contains sequences from the Dipterans, the previously identified *Tribolium* tor ortholog, as well as orthologs from *Bombyx*, two ant species (*C. floridanus* and *A. echinatior*), *Nasonia* and *A. pisum* (Shigenobu et al., 2010) (Fig. 1B). This group also included a single protein from the chelicerate *Ixodes*, but no ortholog of tor was found in the genome of the spider-mite (*T. urticae*).

Orthologs of *tsl* were identified from every insect species examined and the non-insect arthropod *D. pulex* (Fig. 1C). No ortholog of *tsl* could be identified in either of the chelicerate genomes indicating that *tsl* likely evolved in the pan-crustacean lineage. There are two paralogs of *tsl* in the pea aphid genome (Shigenobu et al., 2010). Phylogenetic analysis indicates that one of these is highly diverged and groups with the *Daphnia* sequence (likely a result of long branch attraction), we refer to the derived copy of the aphid *tsl* gene as *torso-like related* (*Ap-tslr*). A second copy of *Ap-tslr* can be detected in the pea aphid genome, however, as it is almost identical at the nucleotide level it is likely to be a very recent duplication event or a genome assembly error, and cannot be specifically detected by RT-PCR (data not shown).

Torso-like has divergent expression patterns in insect ovaries

Despite being the most widely conserved component of the terminal-patterning pathway (Fig. 1C), *tsl* RNA is detected in distinct patterns and cell types in the ovaries of insects.

Consistent with previously published data (Martin et al., 1994; Savant-Bhonsale and Montell, 1993). *Dm-tsl* RNA is detected in the border cells at the anterior of the egg chamber and the posterior follicle cells at the posterior of the egg chamber (Fig. 2A). Later in oogenesis *Dm-tsl* RNA is also detected in the centripetal cells adjacent to the anterior end of the oocyte (Fig. 2B). It is this spatial restriction of *Dm-tsl* that is thought to confer spatial specificity to the terminal-patterning pathway (Savant-Bhonsale and Montell, 1993). To determine whether the orthologs of *tsl* we have identified in the pea aphid and the honeybee also have spatially restricted expression, and therefore may have a role in terminal patterning, we examined the maternal expression of *tsl* by *in situ* hybridization.

In honeybee queen ovaries *Am-tsl* RNA is detected in the cytoplasm and nuclei of the posterior nurse cells at stage 3 of oogenesis (arrowhead Fig. 2C). By stage 6 of oogenesis *Am-tsl* RNA is detected in all of the nurse cells (double arrowhead Fig. 2C). As the oocytes mature (stage 7) the nurse cell cluster associated with the mature oocyte degenerates and *Am-tsl* RNA is detected weakly in the degrading nurse cells (asterisk in Fig. 2C). *Am-tsl* RNA is not maternally deposited into the oocyte, nor detected in follicle cells (see enlargement in Fig. 2C), and its expression is not polarized. It is unlikely, therefore, to have a role in axis specification, or to confer spatial orientation to the developing oocyte.

Am-tsl is, however, likely to have a role in active oogenesis as *Ap-tsl* RNA is detected in the ovaries of actively reproducing queen bees (Fig. 2C) and reproductively active (queen-less) worker bees (Fig. 2E), but not reproductively inactive (queen-right) worker bees (Fig. 2D). In worker bees, irrespective of their reproductive status, *Ap-tsl* RNA is also detected in the ovarian duct, indicating a possible additional function in this tissue.

The pea aphid can reproduce sexually (oviparously) or asexually (viviparously) dependent on temperature and day length. These two modes of embryogenesis produce morphologically identical adults, yet there are substantial differences in developmental environment. Sexually produced embryos develop inside a yolk filled egg, whilst asexually produced embryos develop inside their mother and are born live as nymphs (Le Trionnaire et al., 2008). We have previously shown that there are differences in the expression of axis patterning genes between sexually and asexually produced embryos, implying the existence of two different developmental programs in the same genome (Duncan et al., in press). Hence we describe expression patterns of genes related to terminal patterning in both sexual (oviparous) and asexual (viviparous) aphids.

In aphids, *Ap-tsl* RNA is detected in maternal tissue of both sexual (oviparous) and asexual (viviparous) ovaries, but in different expression patterns. In asexual ovaries, where embryonic development occurs within the mothers abdomen, *Ap-tsl* RNA is not detected in either the nurse or follicle cells as the oocyte develops, nor is it detected during early embryogenesis (Fig. 2F). However, as the germ band begins to invaginate, *Ap-tsl* RNA is detected in the maternal follicle cells at the posterior of the stage 9 embryo (Fig. 2G and H). This expression is transient and is not detected at stage 12 as the germ band elongates (Fig. 2I). No further maternal expression of *Ap-tsl* RNA is observed until late in embryogenesis, when at stage 17 *Ap-tsl* RNA expression is again observed in the posterior follicle cells (Fig. 2J). At this stage, strong staining is seen in the follicle cells separating the most mature embryo from the entry to the lateral oviducts (Fig. 2K).

In oviparous (sexual) ovaries, *Ap-tsl* RNA is weakly maternally expressed. However, as in seen in viviparous ovaries the strongest expression is in the posterior follicle cells late in oogenesis as the oocyte matures. The expression of *Ap-tsl* in these follicle cells initiates after the yolk begins to be deposited (compare Fig. 2L and M with Fig. 2N and O). Just prior to *Ap-tsl* RNA being detected

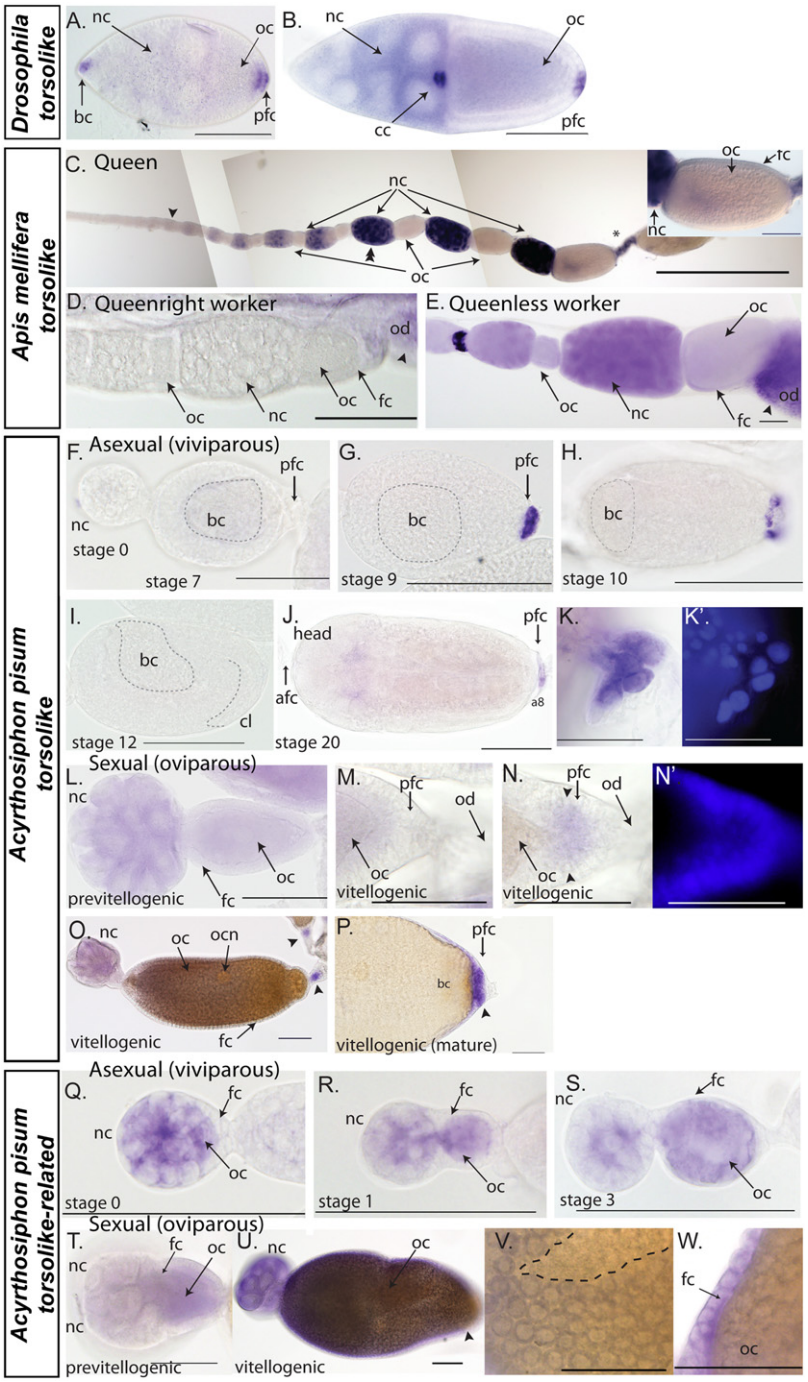

Fig. 2. *Torso-like* is expressed in different cells of *Drosophila*, honeybee and aphid ovaries: (A) in *Drosophila, tsl* RNA is detected in the posterior follicle cells and the border cells at stage 9 of oogenesis. (B) At stage 10 of oogenesis *Dm-tsl* RNA is detected in the centripetal cells and posterior follicle cells. (C) In reproductively active honeybee queen ovaries *Am-tsl* RNA is initially detected in posterior nurse cells at stage 3 of oogenesis (arrowhead). By stage 6 *Am-tsl* RNA is found ubiquitously throughout the nurse cell cluster (double arrowhead), but is not maternally provided by the oocyte and is not detected in follicle cells (refer to inset for higher magnification of follicle cells). As the oocyte matures (at stage 7), the nurse cells atrophy (indicated by an asterisk) and *Am-tsl* RNA dissipates. Scale bar = 1 mm and 100 μm in inset. (D) In reproductively inactive worker honeybee ovaries *Am-tsl* RNA is not detected in the ovariole, but *Am-tsl* RNA is detected in the ovarian duct (arrowhead). (E) In reproductively active honeybee workers *Am-tsl* RNA is detected in a similar expression pattern to that seen in queens; *Am-tsl* RNA is detected throughout the nurse cell cluster, but is not maternally deposited into the oocyte, and it is not detected in the follicle cells. *Am-tsl* RNA is also detected in cells of the ovarian duct. (F) In the pea aphid *Ap-tsl* RNA is not detected in viviparous (asexual) oocytes, nor in the early stages of embryogenesis. (G) At stage 9 after incorporation of the endosymbiotic bacteria *Ap-tsl* RNA is detected in the enlarged follicle cells at the posterior of the embryo. (H) Expression in the posterior follicle cells persists until stage 10. (I) No *Ap-tsl* RNA is detected in the posterior follicle cells as the embryo matures. (J) At stage 20, as the embryo reaches maturity, *Ap-tsl* RNA is again detected in the posterior follicle cells immediately adjacent to the ovarian duct. (K) Higher magnification image of posterior follicle cells that have been disassociated from the ovarian duct. Clear staining for *Ap-tsl* RNA can be seen associated with these cells. Scale bar = 50 μm. (L) *Ap-tsl* RNA is detected weakly in the nurse cell cluster of previtellogenic oviparous (sexual) oocytes. (M) No *Ap-tsl* RNA can be detected in the posterior follicle cells as vitellogenesis begins. Scale bar = 50 μm. (N) As the posterior follicle cells undergo a change in morphology *Ap-tsl* RNA is detected in a sub-set of these cells flanking the oocyte (arrowheads). Scale bar = 50 μm. (O) After the onset of vitellogenesis *Ap-tsl* RNA can be detected in the nurse cell cluster but strongest expression is seen in the posterior follicle cells (arrowhead). (P) As the oocyte matures *Ap-tsl* RNA persists in the posterior follicle cells. Scale bar = 50 μm. (Q) RNA for *Ap-tslr* is maternally provided to stage 0 oocytes in viviparous (asexual) ovaries. (R) Maternal expression persists throughout oogenesis. (S) By stage 3 *Ap-tslr* RNA remains ubiquitous within the oocyte and is not localized. *Ap-tslr* RNA is not detected in the follicle cells at any of these stages. (T) In oviparous ovaries, prior to vitellogenesis, *Ap-tslr* RNA weakly maternally provided to the developing oocyte. (U) After the onset of vitellogenesis, *Ap-tslr* RNA is detected strongly in all of the follicle cells overlying the developing oocyte. (V) High magnification image showing an area where follicle cells have been removed to demonstrate that staining for *Ap-tslr* RNA is in the follicle cells and is barely detectable in the oocyte. (W) High magnification image showing a lateral view of the follicle cell layer, demonstrating high levels of staining for *Ap-tslr* RNA, whilst virtually no staining is detected in the oocyte. Scale bars indicate 100 μm unless otherwise stated. Abbreviations: afc = anterior follicle cells, bc = bacteriocyte, bc = border cell, cc = centripetal cell, fc = follicle cell, nc = nurse cell, od = ovarian duct, oc = oocyte, pfc = posterior follicle cells.

the posterior follicle cells undergo a change in morphology. The follicle cells at the posterior enlarge causing thickening and apparent elongation of the connection between the oocyte and the ovarian duct (compare Fig. 2M and N). Expression of *Ap-tsl* persists in the most posterior follicle cells, adjacent to the ovarian duct, until the oocyte matures (Fig. 2P).

The second *tsl* ortholog found in the pea aphid, *Ap-tslr*, has a distinct expression pattern. *Ap-tslr* RNA is maternally expressed in both viviparous (asexual) oocytes (Fig. 2Q–S) and pre-vitellogenic oviparous (sexual) oocytes (Fig. 2T). However, in sexual (oviparous) oocytes *Ap-tslr* RNA is strongly detected in the follicle cells surrounding the developing oocyte after yolk begins to be deposited (Fig. 2U, W, and V). Expression persists in theses follicle cells until the oocyte reaches maturity. It is difficult to determine from these *in situ* hybridizations whether *Ap-tslr* RNA accumulates appreciably within the oocyte. RT-PCR of unfertilized mature oocytes detects very low levels of *Ap-tslr* transcripts (Supplementary Fig. 3), which is consistent with the expression of *Ap-tslr* in follicle cells rather than accumulation within the developing oocyte.

Based on these expression patterns it appears that *Am-tsl* RNA does not have spatially restricted expression, but *Ap-tsl* RNA does; it is expressed in the posterior follicle cells during embryogenesis in asexual (viviparous) aphids, and in the posterior follicle cells late in sexual (oviparous) oogenesis. In contrast, *Ap-tslr* does not spatially restrict expression.

Expression of tsl in insect embryos

Given the different patterns of *tsl* expression we observed in the ovaries of honeybees, *Drosophila* and aphids (Fig. 2), we wanted to determine whether tsl may play another, more conserved, role during development. Indeed it has been shown that tsl also has a role in tor/PTTH signaling in the prothoracic gland (Grillo et al., 2012). We therefore examined the expression of *tsl* during embryonic development by *in situ* hybridization.

In early *Drosophila* embryos *Dm-tsl* mRNA is detected first at stage 7, in cells of the procephalic neurogenic ectoderm, an expression pattern that has not been previously reported (Fig. 3A). Expression in this region persists until stage 11 when *Dm-tsl* is expressed in cells of the ventral midline, likely the midline glia (Fig. 3B and C) (Martin et al., 1994).

In the honeybee, RNA for *Am-tsl* is not detected early in embryogenesis (data not shown). Late in embryogenesis *Am-tsl* is detected in patches of cells flanking the ventral midline (Fig. 3D). Strong staining is detected in a patch of cells in each embryonic segment from the 3rd thoracic segment to the most posterior abdominal segment (Fig. 3E). The timing and location of expression suggests that these may be tracheal placodes (Wilk et al., 1996). Staining for *Am-tsl* is also detected in bilateral patches of cells in the cerebrum of the embryo, anterior to the mandibular segment (Fig. 3E′).

In aphids, *Ap-tsl* is not detected early in embryogenesis in either viviparous or early oviparous embryos (data not shown). Embryonic expression of *Ap-tsl* RNA is detected until stage 16 of embryogenesis, after the germband is fully extended and the embryo has flipped as a result of katatrepsis. At stage 16 *Ap-tsl* RNA is detected in four patches of cells anterior to the first thoracic segment (Fig. 3F). These expression domains elongate during stage 16 towards the midline of the animal (Fig. 3G). An additional patch of cells posterior to the initial expression domains, expresses *Ap-tsl* RNA at stage 17 (Fig. 3H). The expression domains of *Ap-tsl* continue to elongate towards the lateral surface of the embryo (Fig. 3I) resolving at stage 20 into two complex swirls of cells expressing *Ap-tsl* RNA (Fig. 3J). The cells expressing *Ap-tsl* RNA extend towards the dorsal surface of the animal (Fig. 3K and L).

Ap-tslr RNA is initially detected at stage 11 of embryogenesis in viviparous (asexual) embryos. At this stage *Ap-tslr* RNA is present diffusely in cells near the bacteriocyte (the specialized cells that house the obligate endosymbiont *Buchnera aphidicola* (Braendle et al., 2003)) and in a stripe of cells in a position adjacent to the developing cephalic lobe and bisecting the presumptive thorax tissue (Fig. 3M). At stage 12 *Ap-tslr* RNA is associated with cells adjacent to the bacteriocyte and appears to overlap with the presumptive germ cells (Fig. 3N) (Chang et al., 2007). *Ap-tslr* RNA continues to be detected in cells adjacent to the bacteriocyte as the bacteriocyte is pushed to the anterior pole as a result of germ band extension (Fig. 3O). By late stage 14 *Ap-tslr* RNA is detected in cells adjacent to and covering the bacteriocyte (Fig. 3P) at this stage *Ap-tslr* RNA is also detected in bilateral diffuse stripes of cells running along the dorsal surface of the embryo. The expression domain extends from the second thoracic segment through to the fifth abdominal segment. As the embryo flips (katatrepsis) weak staining for *Ap-tslr* RNA is detected in the germ cells as they reach their final position (Fig. 3Q). *Ap-tslr* RNA is also detected in eight patches of cells along the lateral surface of the embryo. The positions of these cells correspond with the thoracic segments and first five abdominal segments. The timing and location of *Ap-tslr* RNA suggests that these cells may be tracheal placodes, similar to the staining seen for *Am-tsl* (Fig. 3D). In mature embryos (stage 20) *Ap-tslr* RNA is only detected in the ovaries associated with the nurse cell clusters and developing oocytes (Fig. 3R).

Based on these expression patterns it appears that there are conserved aspects in the expression of *tsl* during embryogenesis, for instance *Dm-tsl*, *Am-tsl* and *Ap-tsl* are all expressed in regions of the developing brain. However, the details of these expression patterns differ. *Am-tsl* and *Ap-tslr* also appear to be both expressed in the tracheal placodes, possibly suggesting a conserved role for *tsl* in these tissues.

Expression of Ap-torso (Ap-tor), Ap-prothoraciotrophic hormone (Ap-PTTH), Ap-Noggin-like1(Ap-NL1), and Ap-Noggin-like2 (Ap-NL2) during aphid oogenesis and embryogenesis

The polarized expression of *Ap-tsl* in the posterior follicle cells adjacent to the developing sexual (oviparous) oocyte raises the possibility that a version of the terminal patterning system may be functional during oviparous oogenesis. To investigate this possibility we examined the expression of *Ap-tor* (Fig. 1B) and in the absence of an ortholog of trk in the pea aphid we also examined the expression of related cys-knot ligands, *Ap-PTTH*, *Ap-NL1* and *Ap-NL2* (Fig. 1A) by *in situ* hybridization.

Bioinformatic analysis identified a possible aphid ortholog of *tor* (Fig. 1B) (Shigenobu et al., 2010). In *Drosophila* and *Tribolium* *tor* RNA is ubiquitously distributed during early embryogenesis (Schoppmeier and Schroder, 2005; Sprenger et al., 1989). However, *in situ* hybridization reveals that *Ap-tor* RNA is not detected in viviparous (asexual) oocytes (Fig. 4A(i)) and is not expressed early in development (Fig. 4A(i) and (ii)). *Ap-tor* RNA is not detected in embryos immediately post-katatrepsis (stage 16, Fig. 4A(iii)), however as the germ band begins to retract at stage 17, *Ap-tor* RNA is detected in paired lateral expression domains within the prothoracic segment that persists until the embryo is mature (Fig. 4A(iv)–(vi)).

Ap-tor RNA is also not detected in oviparous (sexual) ovaries by *in situ* hybridization (Fig. 4B(vii)–(ix)). RT-PCR (Supplementary Figs. 3 and 4) indicates that *Ap-tor* transcripts are present in pre-vitellogenic oviparous oocytes, but it is barely detectable after the onset of vitellogenesis, and is undetectable in mature but

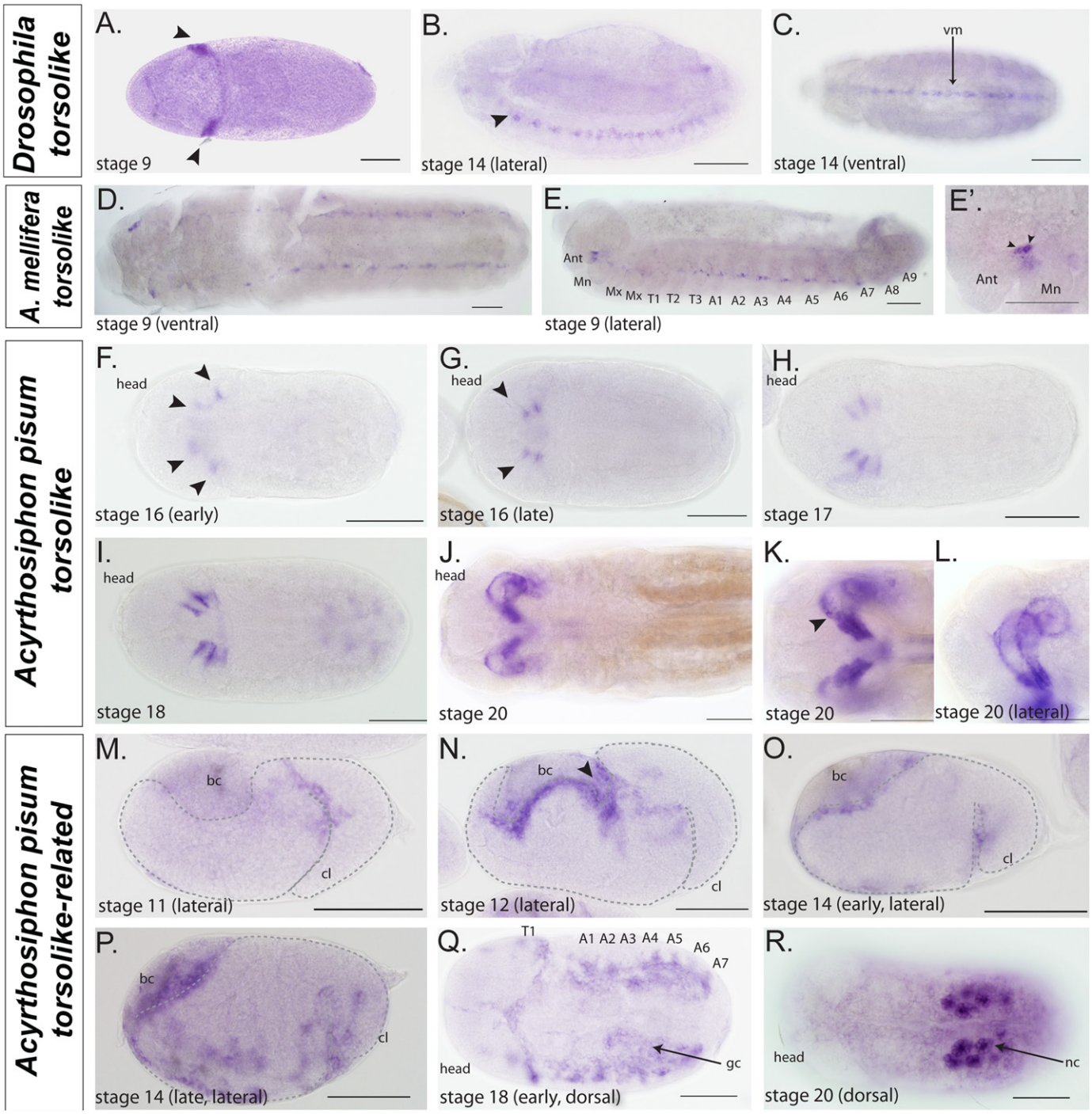

Fig. 3. Torso-like is expressed during different developmental stages in *Drosophila*, the honeybee and the pea aphid: (A) *Dm-tsl* RNA is detected at stage 9 in the visual anlagen, (B) by Stage 11 *Dm-tsl* RNA is detected in cells of the ventral midline, (C) ventral view showing *Dm-tsl* expression in cells of the ventral midline, (D) *Am-tsl* is detected late in embryogenesis in cells flanking the ventral midline, (E) *Am-tsl* RNA is detected in a patch of cells from the 3rd thoracic segment to the most posterior abdominal segment. Paired expression domains are also seen in the cerebrum anterior to the mandibular segment. (E′) Higher magnification image showing expression of *Am-tsl* RNA in two cells anterior to the mandibular segment (arrowheads). (F) In viviparous embryos *Ap-tsl* RNA is first detected in the embryo at stage 16 in two bilateral paired domains (arrowhead). (G) These domains extend towards the lateral surface of the embryo during late stage 16. (H) At stage 17 a third expression domain is detected at the posterior of the two initial expression domains. (I) These domains continue to extend laterally during stage 18. (J) By stage 20 *Ap-tsl* RNA is detected in a complex expression pattern emanating from the initial three expression domains. These swirls of *Ap-tsl* RNA are associated with cells (arrow head in K) and are at different focal planes within the embryo (L). (M) *Ap-tslr* RNA is detected in stage 11 embryos. A diffuse expression domain is seen near to the bacteriocyte and a stripe of cells next to the presumptive cephalic lobe also expresses *Ap-tslr* RNA. (N) At stage 12 *Ap-tslr* RNA is associated with cells adjacent to the bacteriocyte (arrowhead indicates the approximate location of the germ cells). (O) This association continues through stage 14. (P) At late stage 14 *Ap-tslr* RNA is detected in cells adjacent to the bacteriocyte and in two tracts of cells running along the ventral surface of the embryo. (Q) At stage 19 as the germ cells reach their final position *Ap-tslr* RNA is detected in the germs cells. *Ap-tslr* RNA is also detected in a segmental pattern in patches of cells towards the lateral surface of the embryo. (R) In a mature embryo *Ap-tslr* RNA is associated with the mature nurse cell clusters and developing oocytes. Scale bars=100 μm. All views are ventral unless otherwise specified. Abbreviations:, Ant=antennal segment, bc=bacteriocyte, cl=cephalic lobe, gc=germ cells, Mn=mandibular segment, Mx=maxillary segment, nc=nurse cells, vm=ventral midline.

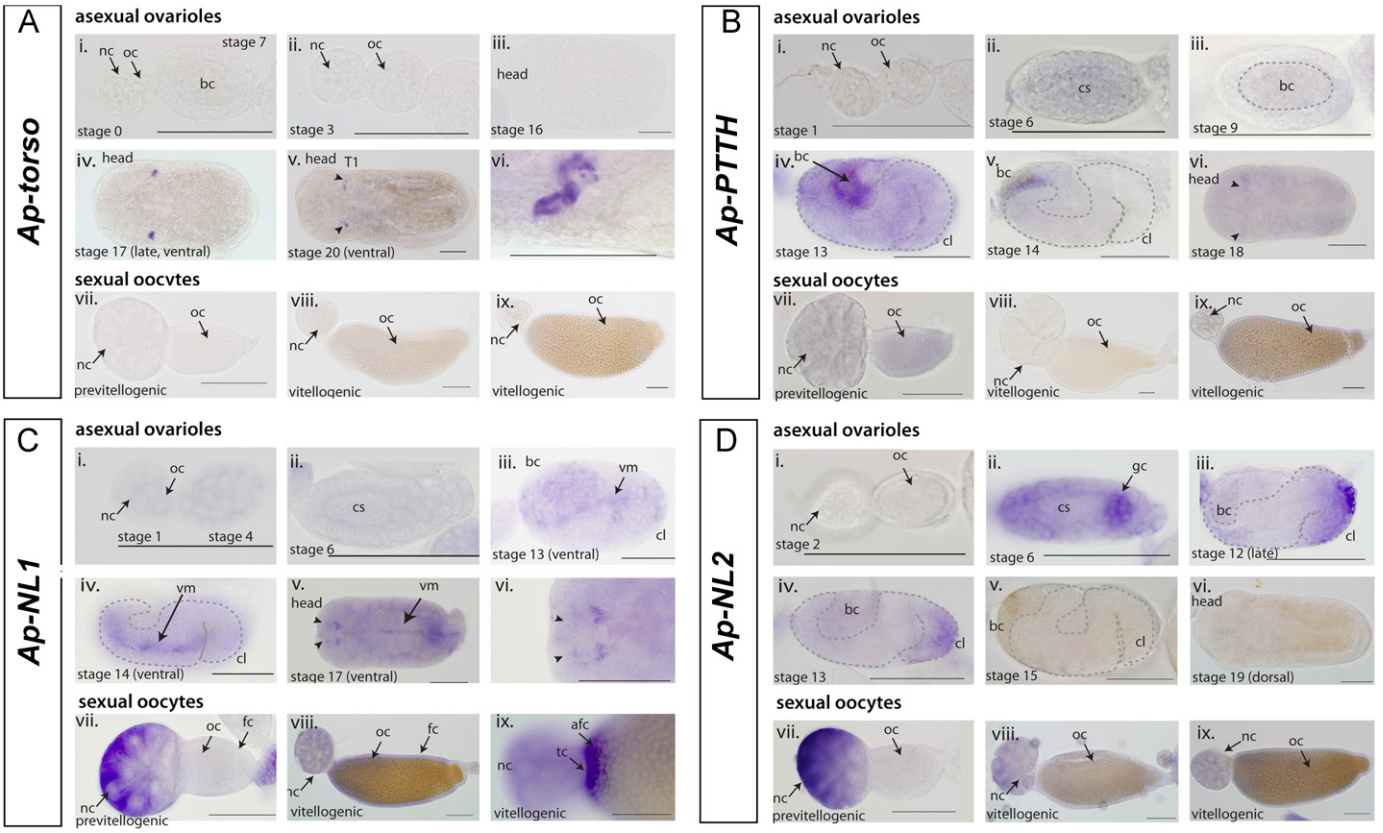

Fig. 4. Expression of *Ap-torso* and *Ap-Noggin-like* during aphid oogenesis and embryogenesis: (A) *in situ* hybridization for *Ap-tor*. (i) *Ap-tor* RNA is not detected in germaria or early viviparous (asexual) oocytes, nor in early embryogenesis. (ii) *Ap-torso* RNA is not detected in stage 3 oocytes. (iii) *Ap-tor* RNA is not detected at stage 16 of embryogenesis. (iv) At late stage 17 *Ap-tor* RNA is detected in paired lateral domains in the first thoracic segment. (v) *Ap-tor* RNA continues to be detected in these domains as the embryo matures. (vi) *Ap-tor* RNA exhibits a spatially complex expression domain. (B) *In situ* hybridization for *Ap-PTTH*. (i) *Ap-PTTH* RNA is not detected during oogenesis in viviparous (asexual) oocytes. (ii) *Ap-PTTH* RNA is not detected during blastoderm stages of embryogenesis. (iii) *Ap-PTTH* RNA is not detected as the endosymbiotic bacteria are incorporated into the embryo. (iv) As the germband elongates *Ap-PTTH* RNA is detected in cells associated with the bacteriocyte. (v) Cells associated with the bacteriocyte continue to express *Ap-PTTH* RNA as the germband pushes the bacteriocyte to the anterior. (vi) In mature embryos *Ap-PTTH* RNA can be detected in paired domains anterior to the first thoracic segment. (C) *In situ* hybridization for *Ap-NL1*: (i) *Ap-NL1* RNA is not maternally provided to the viviparous (asexual) oocyte and is not detected early in embryogenesis (ii). (iii) At stage 13 *Ap-NL1* RNA is enriched in cells of the ventral midline. (iv) *Ap-NL1* RNA is detected in the ventral midline at stage 14 of development. (v) *Ap-NL1* RNA persists in the ventral mid-line until late in development and in mature embryos *Ap-NL1* RNA is detected in two circular patches of cells in the cephalic lobes of the brain. (vi) Higher magnification image showing expression of *Ap-NL1* in the brain of a mature embryo (arrowheads). (vii) *Ap-NL1* RNA is detected in the nurse cell clusters of oviparous (sexual) oocytes, but is not deposited into the oocyte. (viii) At the onset of vitellogenesis *Ap-NL1* RNA is barely detectable in the nurse cell cluster but is expressed in the follicle cells. (ix) As the oocyte matures *Ap-NL1* RNA is enriched in the anterior follicle cells. (D) *In situ* hybridization for *Ap-NL2*: (i) *Ap-NL2* RNA is not maternally provided to the viviparous (asexual) oocyte. (ii) At blastoderm stages *Ap-NL2* RNA is detected in the germ cells as they are being specified. (iii) At stage 12 *Ap-NL2* RNA is detected throughout the presumptive cephalic lobes. (iv) *Ap-NL2* RNA continues to be detected in the cephalic lobes until stage 13. (v) *Ap-NL2* RNA is not detected beyond stage 15 of embryogenesis, nor in mature embryos (vi). (vii) *Ap-NL2* RNA is detected in the nurse cell clusters of oviparous (sexual) oocytes, but is not deposited into the oocyte. Expression of *Ap-NL2* RNA in the nurse cell cluster persists throughout oogenesis (vii)–(ix), but the RNA is not detected in the oocyte nor in the overlying follicle cells. Scale bars = 100 μm. All images are lateral views unless otherwise specified. Abbreviations: afc = anterior follicle cell, bc = bacteriocyte, cs = central syncytium, cl = cephalic lobes, fc = follicle cells, gc = germ cells, nc = nurse cell, oc = oocyte, vm = ventral midline.

unfertilized eggs, consistent with transient expression in the germarium, but not with maternal deposition into the oocyte. These data indicate that maternal *Ap-tor* RNA is not present in either viviparous (asexual) or oviparous (sexual) oocytes and therefore cannot be functioning in canonical terminal-patterning in the pea aphid.

PTTH and trk share some sequence similarity (Fig. 1A) (Grillo et al., 2012; Rewitz et al., 2009) and *tor* has been demonstrated to be the receptor for PTTH in *B. mori* (Rewitz et al., 2009). PTTH over-expression has also been demonstrated to partially rescue the terminal phenotype of *Drosophila* trk[1] mutants (Rewitz et al., 2009) demonstrating that PTTH can function as the ligand for tor, initiate MAPK signaling and affect the expression of downstream targets including *tll*. This raises the possibility that, in the absence of trunk, Ap-PTTH may function as a ligand for terminal patterning in the pea aphid. However, *Ap-PTTH* (ACYPI37989) is virtually undetectable by RT-PCR (Supplementary Fig. 4), and is present at low levels in viviparous ovarioles (containing asexually produced embryos of different developmental stages) and very low levels in pre-vitellogenic oviparous (sexual) ovarioles. Using *in situ* hybridization we do not detect *Ap-PTTH* RNA in the nurse cell clusters or oocytes of viviparous (asexual) oocytes (Fig. 4B(i)), nor in blastoderm stage embryos (Fig. 4B(ii). No RNA for *Ap-PTTH* can be detected as the endosymbiotic bacteria are incorporated into the bacteriocyte (Fig. 4B(iii), but as the bacteriocyte is shifted towards the posterior of the embryo as a result of germ band elongation, *In situ* hybridization reveals weak expression of *PTTH* by cells surrounding the bacteriocyte (Fig. 4B(iv)). This expression domain is relatively transient (Fig. 4B(v)). In mature embryos very weak staining for *Ap-PTTH* can be detected in mature embryos towards the dorsal surface of the embryo adjacent to the first thoracic segment (Fig. 4B(vi)). No expression of *Ap-PTTH* RNA was detected in the brain. However, this may be due to poor probe penetration, or transient expression of *PTTH*. In oviparous (sexual) ovaries *Ap-PTTH* RNA is very weakly detected in the nurse cell cluster prior to vitellogenesis (Fig. 4B(vii)). Following vitellogenesis some

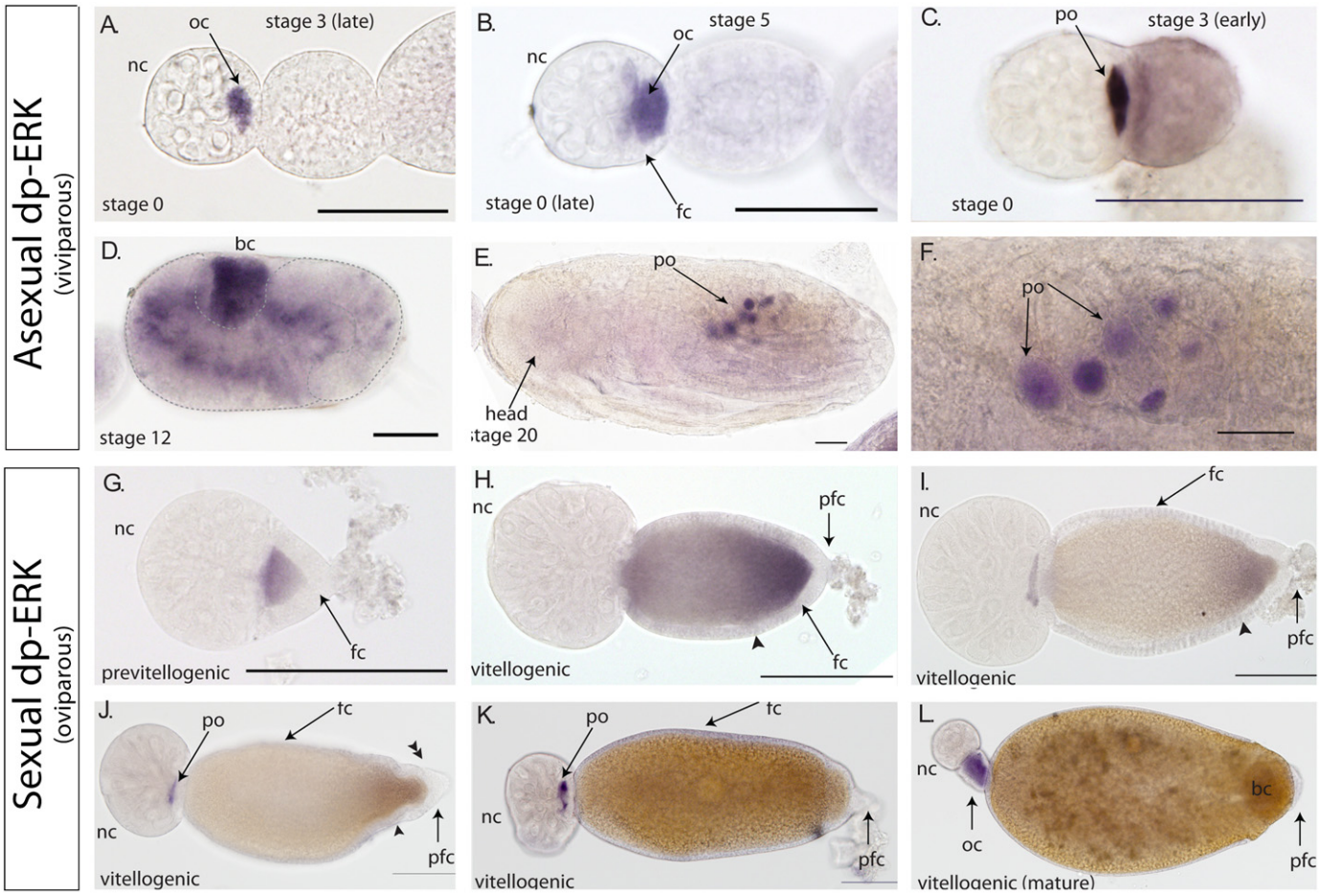

Fig. 5. Activation of MAPK signaling in viviparous and oviparous oocytes: (A) immunohistochemistry for dp-ERK reveals ubiquitous staining in the viviparous (asexual) oocyte. (B) Ubiquitous staining for dp-ERK is seen as the oocyte is specified and as it segregates from the germarium. (C) As the oocyte undergoes a maturation division to initiate embryogenesis dp-ERK staining becomes less intense and diffuse throughout the oocyte. (D) By stage 12 high levels of dp-ERK activation are observed in the bacteriocyte. (E) In mature embryos dp-ERK activation is restricted to the oocytes as they are specified in the fully developed ovary. (F) Higher magnification image showing the prospective oocytes in a mature embryo. (G) In previtellogenic oviparous (sexual) ovaries dp-ERK is ubiquitously activated throughout the early oocyte. (H) At the onset of vitellogenesis dp-ERK begins to clear from the anterior of the oocyte, possibly due to the deposition of yolk. (I) Staining for dp-ERK is cleared rapidly from the oocyte in an anterior to posterior sequence. (J) In early-vitellogenesis dp-ERK staining is restricted to the posterior pole of the oocyte (arrowhead). At this stage the posterior follicle cells begin to change their morphology (double arrowhead). (K) No staining for dp-ERK is observed in the oocyte during mid-vitellogenesis. (L) No dp-ERK staining is observed in mature oocytes. Scale bars = 100 μm. All images are lateral views. Abbreviations: bc = bacteriocyte, fc = follicle cell, nc = nurse cell, oc = oocyte, po = prospective oocyte.

residual staining can be detected (Fig. 4B(viii)), but *Ap-PTTH* RNA is no longer detected in the nurse cells (Fig. 4B(vii)–(ix)).

The absence of *Ap-PTTH* RNA during viviparous (asexual) or oviparous (sexual) oogenesis means that *Ap-PTTH* cannot be functioning as a ligand for the terminal patterning pathway. However, phylogenetic analyses (Fig. 1A, Supplementary Fig. 2) also revealed similarity between trk and a second class of proteins, the NL proteins. Two NL proteins were found in the pea aphid: Ap-Noggin-like1 (Ap-NL1, ACYPI007216) and Ap-Noggin-like2 (Ap-NL2, ACYPI53658). To determine whether these genes may have a role in terminal patterning the expression of these genes was examined by *in situ* hybridization (Fig. 4C and D).

Ap-NL1 RNA is not detected in the viviparous oocyte, or in the blastoderm stage embryos (Fig. 4C). Later in embryogenesis, as the central nervous system develops, *Ap-NL1* RNA is detected in cells of the ventral midline in a similar pattern to *Ap-orthodenticle* (Fig. 4C(iii)) (Duncan and Dearden, 2010; Huang et al., 2010). *Ap-NL1* RNA continues to be detected in this domain until late in development (stage 18, Fig. 4C(iv)), when two semicircular patches of cells expressing *Ap-NL1* RNA are detected in the brain (Fig. 4C(v)–(vi)).

Ap-NL1 RNA is detected in the nurse cells of oviparous oocytes, but *Ap-NL1* RNA is not detected in the previtellogenic oocyte, suggesting that the RNA is not maternally provided to the oocyte (Fig. 4C(vii)). After the onset of vitellogenesis *Ap-NL1*RNA is detected in follicle cells and appears to diminish in the nurse cells (Fig. 4C(viii)). As the oocyte matures the follicle cells at the anterior of the oocyte adjacent to the trophic cord are enriched for *Ap-NL1* RNA (Fig. 4C(ix)).

Ap-NL2 RNA is not detected in the viviparous oocyte (Fig. 4D(i)). At blastoderm stage, *Ap-NL2* RNA is transiently detected in the presumptive germ cells (as determined by comparison with *Ap-nanos1* expression (Duncan et al., 2013; Chang et al., 2009)) (Fig. 4D(ii)). *Ap-NL2* RNA is then transiently detected in the developing brain during embryonic stages 12 and 13 (Fig. 4D(iii) and (iv)). No expression is detected after this stage of embryogenesis (Fig. 4D(v)–(vi)).

In oviparous ovaries *Ap-NL2* RNA is detected strongly in the nurse cells of previtellogenic oocytes (Fig. 4D(vii)), however, there is no evidence that this RNA is deposited into the developing oocyte. As vitellogenesis is initiated *Ap-NL2* is only weakly detected in the nurse cells (Fig. 4D(viii)), and is no longer detectable as the oocyte reaches maturity (Fig. 4D(ix)).

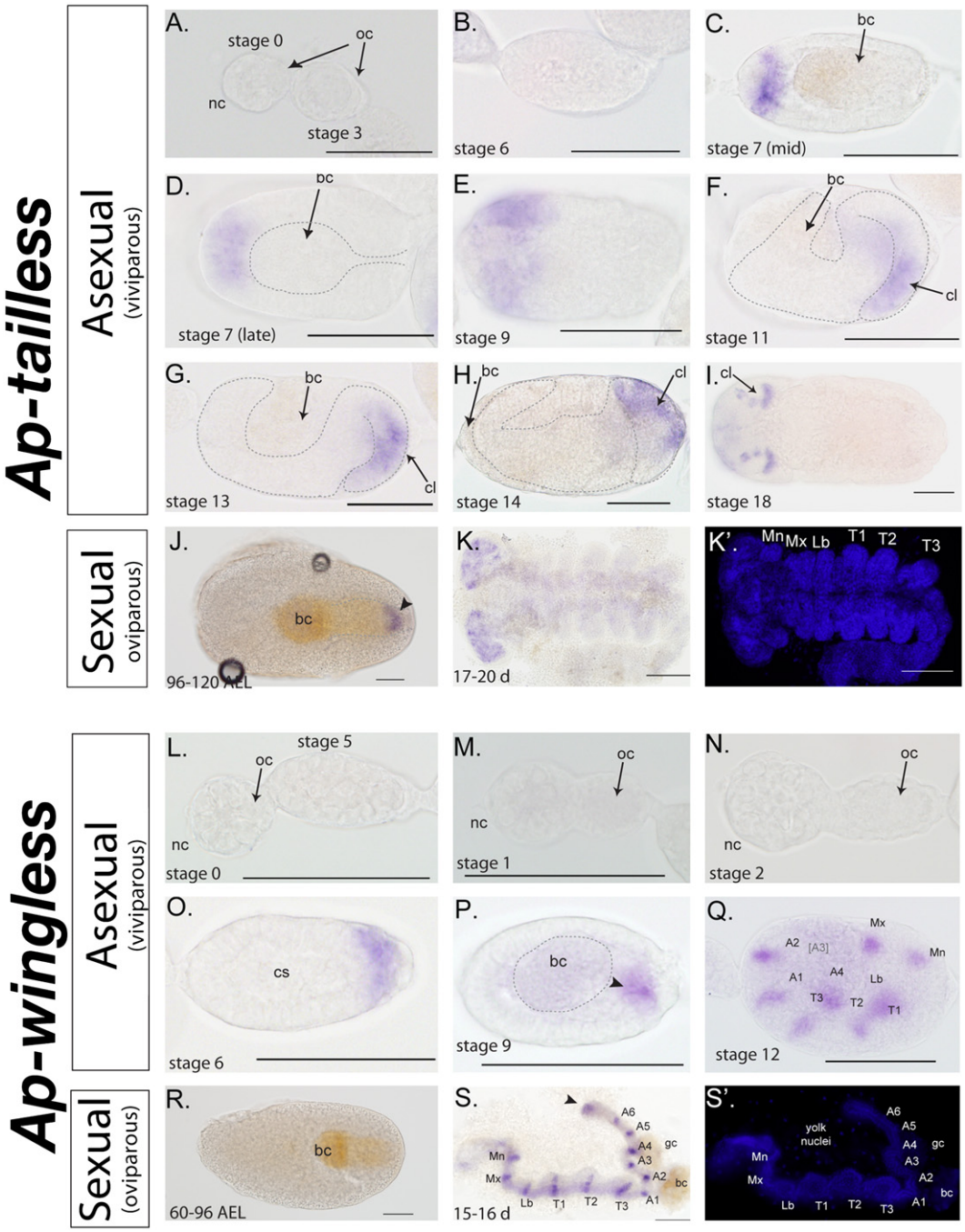

Fig. 6. *Ap-tailless* and *Ap-wingless* are not expressed early in embryogenesis in oviparous or viviparous oocytes: (A) *Ap-tll* RNA is not detected during oogenesis or in blastoderm stage viviparous (asexual) embryos (B). (C) As the endosymbiotic bacteria are incorporated and the germband begins to invaginate *Ap-tll* RNA is detected in an anterior stripe. (D) *Ap-tll* RNA is observed in a cap of expression at the anterior pole. (E) The cap of *Ap-tll* RNA widens to a stripe as anatrepsis is completed. (F) At stage 13 *Ap-tll* RNA is detected in the presumptive cephalic lobe at the anterior of the germ band. (G) *Ap-tll* RNA continues to be detected in the cephalic lobes as the germ band continues to elongate and limb buds are specified. (H) *Ap-tll* RNA is expressed in the cephalic lobes in the extended germ band embryo. (I) In mature embryos (stage 18) *Ap-tll* RNA is detected in semicircular bilateral patches of cells in the brain of the mature embryo. (J) *Ap-tll* RNA is detected at the anterior of the invaginating germband in oviparous (sexual) embryos. (K) *Ap-tll* RNA is detected in the developing brain of extended germ band stage oviparous germ bands that have been dissected from the developing egg. Corresponding DAPI image is shown in K′. (L) *Ap-wg* RNA is not maternally provided in stage 0 viviparous (asexual) oocytes and is not detected in early blastoderm embryos. (M) *Ap-wg* RNA is not detected in stage 1 oocytes, or segregated (stage 2) oocytes (N). (O) At late blastoderm stage *Ap-wg* RNA is detected in a posterior cap of expression, in cells that will form the posterior growth zone. (P) *Ap-wg* RNA is detected in the leading edge of the invaginating germ band. (Q) At stage 12 *Ap-wg* RNA is detected in pattern consistent with a segment polarity gene. (R) *Ap-wg* RNA is not detected in oviparous (sexual) embryos as the germ band elongates. (S) *Ap-wg* RNA is detected in dissected oviparous germ bands in a segment polarity gene expression pattern. Scale bars = 100 μm. Abbreviations: bc = bacteriocyte, cl = cephalic lobe, gc = germ cells, Lb = labrum, Mn = mandibular segment, Mx = maxillary segment, nc = nurse cell, oc = oocyte,

Our data thus shows that even though *Ap-tsl* RNA is expressed by the posterior follicle cells adjacent to the maturing oocyte, we are unable to detect RNA for the receptor (tor) or putative ligands (PTTH, NL1 and NL2). This implies that the canonical terminal-patterning pathway is not active in the pea aphid.

Activation of MAPK signaling during aphid oogenesis and embryogenesis

Activation of the terminal patterning pathway in *Drosophila* results in an intracellular Ras-Raf-MAP-K/Erk phosphorylation cascade that

can be detected at the poles of the embryo by immunohistochemistry with a cross reacting antibody against diphosphorylated ERK (dp-ERK) (Gabay et al., 1997; Lynch et al., 2010; Rousso et al., 2010; Wilson and Dearden, 2009). To determine whether dp-ERK is phosphorylated asymmetrically during pea aphid embryogenesis and oogenesis we performed immunohistochemistry with a cross reacting antibody against dp-ERK.

In viviparous (asexual) aphid ovaries, strong staining for dp-ERK is detected in the developing oocyte at stage 0 (Fig. 5A), before the separation of the oocyte from the germarium (Fig. 5B). Activation of ERK is not spatially restricted within the stage 0 oocyte and therefore does not appear to confer positional information to the developing oocyte. There is no indication of localized dp-ERK activation as the oocyte separates from the germarium or as the maturation division takes place and embryogenesis begins (Fig. 5C), no staining is seen in blastoderm stage embryos (Fig. 5B). No specific staining is seen in the embryos until stage 12, where there is strong staining for dp-ERK is seen in cells associated with the bacteriocyte (Fig. 5D). In mature embryos (stage 20) staining for dp-ERK can be observed in the developing oocytes of the mature ovary (Fig. 5E and F).

Similarly, dp-ERK can be detected in the developing oocyte in oviparous (sexual) ovaries (Fig. 5G). Staining is observed initially ubiquitously through the oocyte beginning after differentiation of the oocyte from the nurse cell population is complete (Fig. 4H). Staining is relatively strong and ubiquitous throughout the oocyte prior to vitellogenesis, but as yolk is detected in the oocyte the staining is diminished, and appears largely restricted to the posterior pole (Fig. 5H and I). Restriction of dp-ERK staining to the posterior pole occurs before any morphological changes are observed in the posterior follicle cells (Fig. 5H and I). As vitellogenesis nears completion dp-ERK staining is reduced and is virtually undetectable as the posterior follicle cells undergo morphological changes (Fig. 5J). As the oocyte reaches maturity dp-ERK staining is undetectable (Fig.5K and L). Immunohistochemistry of freshly laid eggs showed no activated dp-ERK staining early in embryogenesis (data not shown).

Expression of the targets of canonical terminal patterning in the pea aphid: tailless (tll) and wingless (wg)

In *Drosophila* the canonical terminal patterning pathway is known to regulate the expression of down-stream target genes; *tailless* (*tll*) and *huckebein* (*hkb*) (Furriols and Casanova, 2003). To determine whether these targets are likely to be also under control of the terminal-patterning pathway in the pea aphid we investigated the expression of *Ap-tll* during sexual and asexual development (Fig. 6) (*hkb* is missing from the pea aphid genome (Shigenobu et al., 2010)). In asexual aphids, *Ap-tll* is expressed later in development than previously reported for other insects including honeybees (Wilson and Dearden, 2009) and *Tribolium* (Schroder et al., 2000). There is no evidence for maternal expression of *Ap-tll* (Fig. 6A), and zygotic expression is first detected in viviparous embryos during early gastrulation (Fig. 6B and C). *Ap-tll* is initially detected in an anterior cap at stage 7 as the endosymbiotic bacteria are incorporated into the bacteriocyte (Fig. 6C and D). RNA in the anterior of the egg chamber persists until approximately stage 9, during which the anterior stripe expands to approximately 5 cells wide (Fig. 6E). During late stage 11 a domain of cells expressing *Ap-tll* is established in the posterior of the egg chamber (Fig. 6F). This posterior expression domain marks the presumptive cephalic region (as determined by comparison with *Ap-otd* expression (Duncan et al., 2013; Huang et al., 2010)), and expression in this region is stable throughout embryogenesis (Fig. 6G and H). By stage 18, expression of *Ap-tll* is refined to cells likely to be the neuroblasts of the procephalic lobes (Fig. 6I). *In situ* hybridization of oviparous (sexual) ovaries and early embryos revealed no evidence for maternal or early embryonic expression of *Ap-tll*. However, as the germ band invaginates and elongates, at approximately 120 h after egg laying, *Ap-tll* RNA is detected in a stripe of cells at the anterior end of the invaginating germ band (Fig. 6J). Late in oviparous embryogenesis, after the germ band has fully extended, RNA for *Ap-tll* is detected in the procephalic lobes (Fig. 6K).

In *Tribolium*, the terminal-patterning pathway is required to set up or maintain the posterior grown zone of the insect, which requires the induction of *wingless* expression (Schoppmeier and Schroder, 2005). *In situ* hybridization in aphids reveals that in viviparous (asexual) embryos, *Ap-wg* RNA is not detected during oogenesis (Fig. 6 L–N) or early embryogenesis (Fig. 6L). *Ap-wg* RNA is initially detected in a posterior cap during cellular blastoderm (Fig. 6O). The expression in this posterior region persists as the endosymbiotic bacteria are incorporated into the embryo and the germ band begins to invaginate (Fig. 6P). This expression precedes the expected segment polarity expression of *wg*, which begins to appear at stage 11 (Fig. 6Q) consistent with the appearance of engrailed stripes (Miura et al., 2003). No RNA for *Ap-wg* is detected in oviparous ovaries, or in blastoderm stage oviparous embryos, or during germ band elongation (Fig. 6R). In late stage oviparous embryos, the segment polarity expression of *Ap-wg* RNA is detected (Fig. 6S).

The expression patterns of *Ap-wg* and *Ap-tll* are not consistent with regulation via a modified terminal-patterning system, and their expression does not coincide, either spatially or temporally, with *Ap-tsl, Ap-tslr* or dp-ERK staining.

Torso-like from Drosophila, the honeybee and the pea aphid have similar biochemical functions

Our data indicates that *tsl* has a role unrelated to the canonical terminal patterning system in insects such as the honeybee and the pea aphid. In order to determine whether the recruitment of torso-like into terminal patterning in *Drosophila* has resulted in a significant change in protein function, we exogenously expressed the *Drosophila*, *Apis* and *Acyrthosiphon* orthologs of tsl (and tslr) in *Drosophila* using the UAS:GAL4 system to drive expression in the ovary. Gain of function mutations (Klingler et al., 1988) or over-expression of terminal patterning genes (Savant-Bhonsale and Montell, 1993) are known to disrupt abdominal segmentation; causing embryos to be shorter and have fewer abdominal segments even though the embryonic termini are essentially normal. The effects of exogenous *tsl* expression on *Drosophila* embryogenesis were determined by comparing markers of terminal patterning (dp-ERK and *tll* expression), dorso-ventral patterning (*zen* expression), and segmentation (eve expression and cuticle preparations), between wild type embryos (Fig. 7A–E) and embryos produced from flies mis-expressing *torso-like* constructs from *Drosophila* (Fig. 7F–M), the honeybee (Fig. 7N–U), and the two *torso-like* genes from the pea aphid; *Ap-tsl* (Fig. 8A–H) and *Ap-tslr* (Fig. 8I–Q).

Over-expression of *Dm-tsl* causes expansion of the dp-ERK staining domain early in development as compared with wild type *Drosophila* embryos (Fig. 7F), resulting in an expansion of the *tll* expression domain at the posterior of the embryo, and the appearance of a second anterior stripe of *Dm-tll* (Fig. 7G) or a broadening of the anterior stripe (Fig. 7H). No differences are seen in *Dm-zen* expression (Fig. 7I). The expansion of the dp-ERK and *tailless* expression domains translates to fusion of eve stripes in the blastoderm embryo (Fig. 7J and K) and a concomitant deletion of abdominal segments in the larvae (Fig. 7L and M). The severity of segment fusion varies; with the majority of embryos displaying fusion of eve stripes 1 and 2, and 5 and 6 (Fig. 7J), whilst more

severely affected embryos have a single stripe of even-skipped expression or two poorly resolved stripes (Fig. 7K). This disruption of segmentation is reflected in the larval cuticle preparations whereby mildly affected larvae show fusion of denticle belts corresponding with the third abdominal segment to the fourth abdominal segment (Fig. 7L). Severely affected embryos have no denticle belts but often display a duplication of posterior terminal structures (Fig. 7M).

Over-expression of either honeybee (Fig. 7N–U) or aphid *torso-like* (Fig. 8A–H) resulted in phenotypes similar to that seen for the over-expression of *Dm-tsl*. These phenotypes included expansion of both dp-ERK activation (Figs. 7N and 8A) and *tll* expression domains (Figs. 7O, P and 8B). The expansion of these expression domains is reflected in fusion of eve stripes 1 and 2, and 5 and 6 (Figs. 7R and 8D), or the appearance of one or two poorly resolved eve stripes (Figs. 7T and 8E). Similar larval phenotypes are

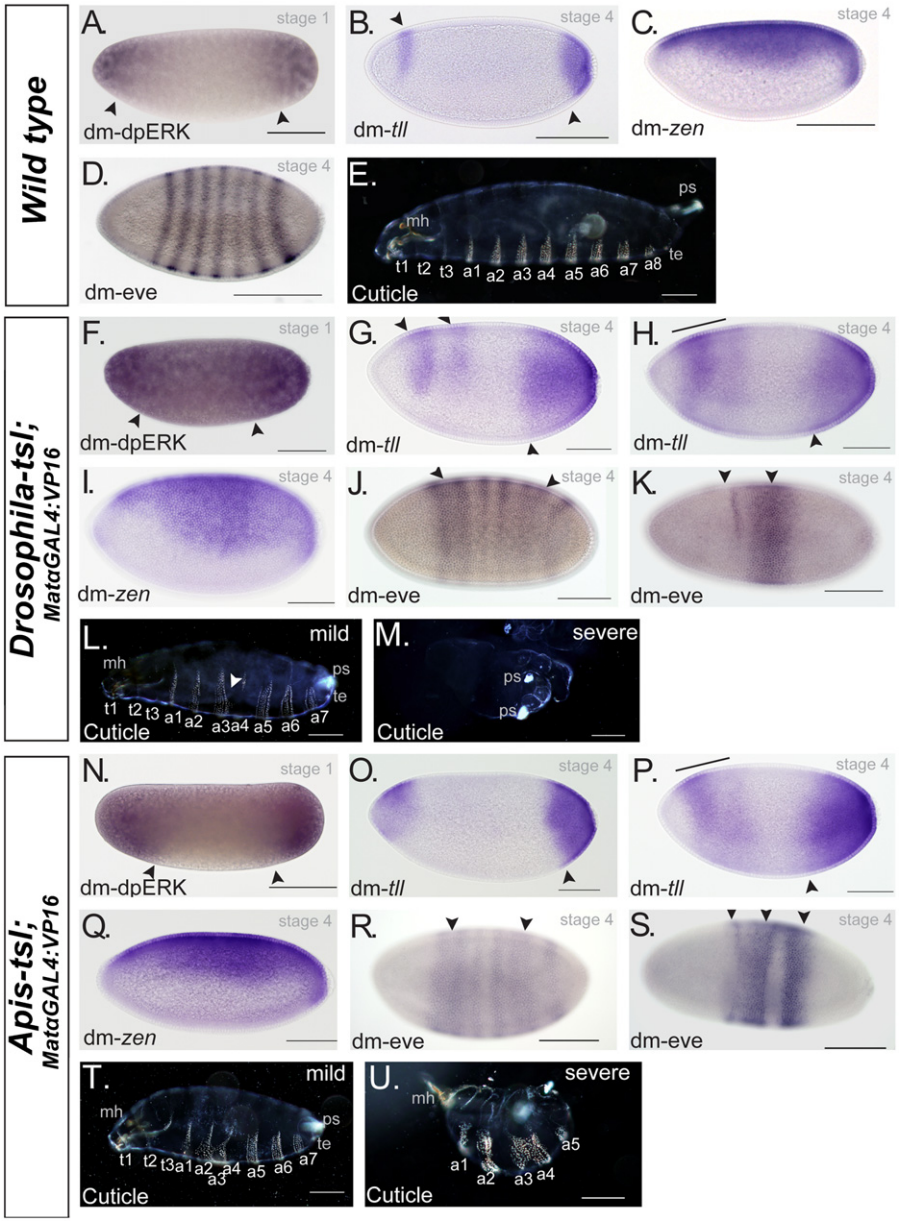

Fig. 7. Ectopic over-expression of *Dm-tsl* and *Am-tsl* in *Drosophila* ovaries. Embryos are oriented to the left and dorsal side is up. The UAS:GAL 4 system was used to drive expression of *torso-like* constructs in the *Drosophila* ovary: (A) immunohistochemistry for dp-ERK in wild type *Drosophila* embryos indicates activation of MAPK signaling at the anterior and posterior poles (arrowheads). (B) In wild type *Drosophila* embryos *Dm-tll* is expressed in an anterior stripe and posterior cap at blastoderm stages (arrowheads). (C) *Dm-zen* is expressed in a dorsal domain, extending down towards the posterior pole in wild type *Drosophila* embryos. (D) Even-skipped protein is observed in 7 distinct stripes in blastoderm stage *Drosophila* embryos. (E) Cuticle of wild-type *Drosophila* larvae. (F) Overexpression of *Dm-tsl* results in expansion of dp-ERK staining domains (arrowheads). (G) *tll* RNA is found in a broad posterior cap and two anterior stripes, which in some specimens equates to a very broad anterior stripe (H). (I) *Dm-zen* RNA is detected in anterior dorsal domains. (J) Dm-eve immunohistochemistry demonstrates fusion of stripes 1 and 2, and 5 and 6. (K) In severely affected embryos Dm-eve protein is observed in a single stripe of cells in the center of the embryo. (L) Cuticle preparations reveal fusion of denticle belts corresponding to the 4th–6th abdominal segments. (M) In severe cases, no denticle belts can be detected and there is an apparent duplication of posterior structures. (N) Overexpression of *Am-tsl* results in expansion of dp-ERK activation at the anterior and posterior poles of the embryo (arrowheads). (O) *Dm-tll* RNA is detected in a broad posterior cap. (P) in severe cases *Dm-tll* RNA is present in a much wider anterior stripe. (Q) No alteration in the expression of *Dm-zen* is observed. (R) Immunohistochemistry for Dm-eve reveals fusion of eve stripes 1 and 2, and 5 and 6 (arrowheads). (S) In severely affected embryos only two poorly resolved stripes of eve are observed (arrowheads). (T) Cuticle preparations reveal fusion of abdominal denticle belts in mild cases. (U) In severely affected cuticles only a few denticle belts are detected. Scale bars = 100 μm.

observed with ectopic overexpression of *Am-tsl* and *Ap-tsl* as that seen with *Dm-tsl*. The larvae are generally shorter, are missing abdominal segments, and fusion is seen of denticle belts A3 and A4 in mildly affected larvae (Figs. 7T and 8F). In moderately affected larvae we see more substantial fusion of the abdominal segments (Figs. 7U and 8G). *Ap-tsl* overexpression also causes head involution defects (Fig. 8H); these defects are fairly common and are observed independently of segmentation defects as several larvae were observed with the segmentation defects seen in Fig. 8G, but with no defects in head involution. These head involution defects are often accompanied by a ventral hole in the cuticle (Fig. 8H), and were not accompanied by changes in the expression of *Dm-zen* (Fig. 8C).

Similar disturbances in embryo patterning were seen with ectopic expression of *Ap-tslr*. The embryos exhibited expansion of dp-ERK activation (Fig. 8I), *tll* expression domains (Fig. 8J and K), and fusion of eve stripes (Fig. 8M and N). However, differences were seen when examining the cuticle preparations. A substantial portion of embryos failed to hatch and three classes of phenotype were observed. The mildest phenotype resembles the over-expression of *Dm-tsl*; there is fusion of abdominal segments A4 and A5, but generally the head and tail structures are normal (Fig. 8O). Embryos with the intermediate phenotype exhibit defects in germband retraction and dorsal closure. They also exhibit substantial defects in head patterning and head involution (Fig. 8P), indicating that ectopic expression of *Ap-tslr* interferes with functions of the late amnioserosa. The most severely affected individuals exhibit improperly formed head structures and in most cases it is difficult to distinguish anterior from posterior. Germ band extension and segmentation are severely affected and individuals usually only have one, or sometimes two incompletely formed denticle belts (Fig. 8Q). This is unlikely to be related to levels of transgene mRNA as the phenotype is identical in two independently generated transgenic lines. This weak ventralizing phenotype is not due to activation of the unfolded protein response (UPR), which has been known to cause a ventralizing phenotype in *Drosophila* embryos, as judged by alternative splicing of *xbp1* (Supplementary Fig. 5). A similar, but much milder

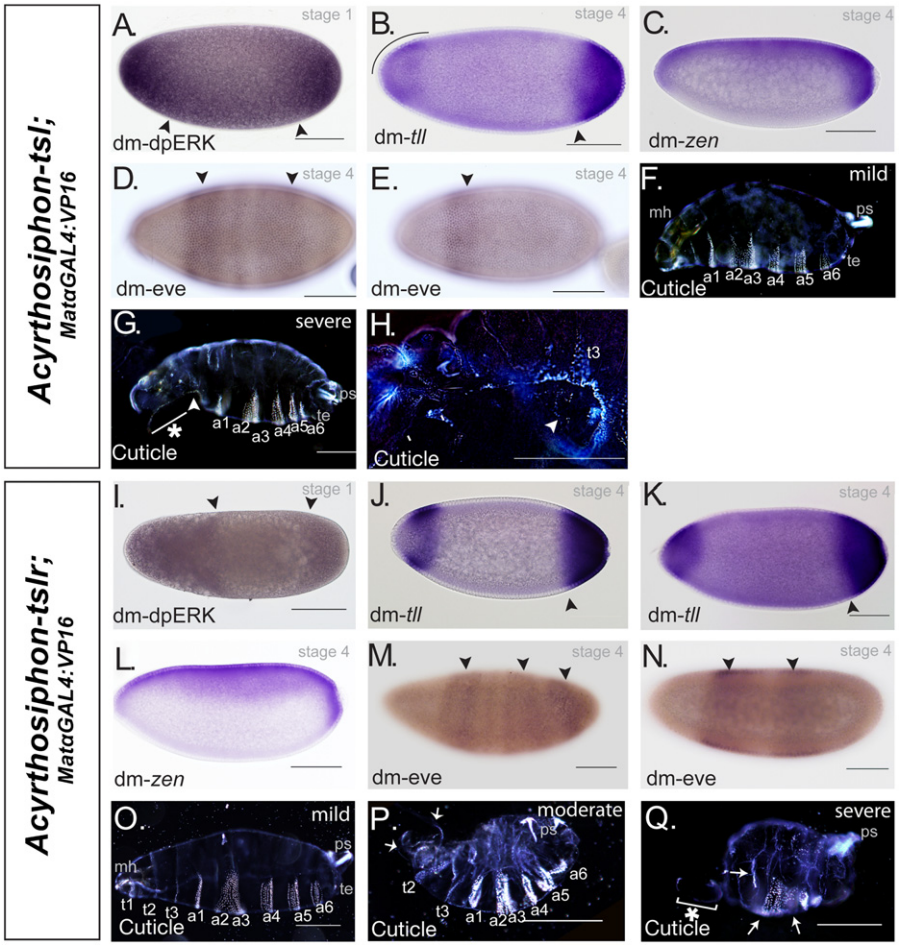

Fig. 8. Ectopic expression of *Ap-tsl* and *Ap-tslr* in *Drosophila* ovaries. Embryos are oriented to the left and dorsal side is up. The UAS:GAL 4 system was used to drive expression of *torso-like* constructs in the *Drosophila* ovary: (A) over-expression of *Ap-tsl* causes expansion of dp-ERK activation domains at the anterior and posterior poles of the embryo (arrowheads). (B) Expansion of the *tll* expression domains is also observed, leading to the expression of *tll* in an anterior cap and a broad posterior cap. (C) no defects in *Dm-zen* expression are observed. (D) Immunohistochemistry for Dm-eve reveals fusion of stripes 1 and 2, and 4–6 (arrowheads). (E) In severely affected embryos only a single stripe of Dm-eve is observed towards the anterior of the embryo. (F) Mildly affected cuticles display a fusion of denticle belts in the abdominal regions. (G) In severely affected individuals the head fails to involute (asterisk in H), and is accompanied by a substantial hole in the ventral cuticle (arrowhead) (H) higher magnification image illustrating a substantial hole in the ventral cuticle. (I) Over-expression of *Ap-tslr* causes an expansion of dp-ERK staining domains (arrowheads). (J) An expansion of *tll* RNA expression is also observed with a broad posterior cap, and an anterior stripe that is shifted towards the anterior. (K) In severely affected embryos *tll* RNA is detected in an anterior cap. (L) No defects are observed with *zen* RNA expression. (M) Immunohistochemistry for eve reveals fusion of stripes 1 and 2, 4 and 5, and 6 and 7 (arrowheads). (N) In severely affected embryos eve protein is detected in two poorly resolved stripes. (O) Mildly affected cuticles show fusion of denticle belts in the abdominal regions. (P) Moderately affected cuticles are shorter, show fusion of denticle belts but also exhibit a head involution defect (arrows), there are also defects in patterning of the posterior termini. (Q) In severely affected cuticles there are one or two incompletely formed denticle belts (arrows) and substantial defects in head patterning (asterisk). Scale bars = 100 μm.

phenotype is seen in *Drosophila* following the over-expression of *zen* (Rafiqi et al., 2010). To determine whether *Ap-tslr* is affecting dorsal closure by expansion of the amnioserosa we examined *Ap-tslr* over-expressing embryos for *zen* expression (Fig. 8L). No differences in *zen* expression were observed between the wild-type and *Ap-tslr* over-expression lines, indicating that *Ap-tslr* is not inducing this severe phenotype by perturbing dorsal-ventral patterning or amnioserosa specification. This suggests that *Ap-tslr* has an activity in *Drosophila* that is independent of its ability to activate torso signaling, and this activity is not present in any other torso-like ortholog tested.

Discussion

Canonical terminal patterning is not active in the honeybee or the pea aphid

The terminal patterning system known from *Drosophila* and *Tribolium* is complex; maternal provision of the RNAs encoding the receptor (torso) and ligand (trunk) are provided to the oocyte during oogenesis, the signal is spatially restricted to the poles of the embryo by the torso-like protein (Casanova et al., 1995; Grillo et al., 2012; Martin et al., 1994; Savant-Bhonsale and Montell, 1993; Schoppmeier and Schroder, 2005; Schroder et al., 2000; Sprenger et al., 1989). Activation of tor signaling causes localized activation of the Ras-Raf-MAP-K/Erk signaling pathway, resulting in the expression of target genes, such as *tailless* and *huckebein* in *Drosophila* and *Tribolium*, and *wingless* and *caudal* in *Tribolium*. Components of this pathway also function in other developmental contexts; torso has been shown to be the receptor for a closely related ligand, PTTH, in *Bombyx* (Rewitz et al., 2009) and *Drosophila*, a process that is thought to require *torso-like* (Grillo et al., 2012).

Here we show that in a basal holometabolous insect (the honeybee) and the hemimetabolous insect (the pea aphid), the canonical terminal patterning system observed in *Drosophila* and *Tribolium* does not appear to be functioning. While the honeybee has an ortholog of *torso-like*, genes encoding *trunk*, *PTTH* and *torso* could not be found in the honeybee genome. This implies that torso-like has a role outside of that regulating the interaction between torso and its ligands in the honeybee.

In the pea aphid genome, orthologs of *torso*, *torso-like* and *PTTH* could be found. However, in viviparous (asexual) embryogenesis *torso* is not maternally provided and *torso* expression is restricted to paired expression domains located in the first thoracic segment of mature embryos. These domains may be in the presumptive prothoracic glands, consistent with an evolutionarily conserved role for PTTH/torso signaling in this gland (Grillo et al., 2012). Consistent with this hypothesis we observe diffuse and weak expression of *PTTH* late in embryogenesis adjacent to the first thoracic segment.

In oviparous (sexual) ovaries, *Ap-tor* RNA is weakly detected by RT-PCR, but RNA is only transiently present, being virtually undetectable post-vitellogenesis and undetectable by oocyte maturity. This expression is consistent with either transient maternal expression of *Ap-tor* or expression in follicle cells surrounding the oocyte, but was undetectable by *in situ* hybridization. This pattern of RNA accumulation differs from *Drosophila* and *Tribolium* where *torso* RNA accumulates at high levels throughout the developing oocyte and is ubiquitous in early embryogenesis when the canonical terminal patterning pathway is active (Schoppmeier and Schroder, 2005; Sprenger et al., 1989).

PTTH can partially rescue *trunk* mutants in *Drosophila* (Rewitz et al., 2009), raising the possibility that PTTH or the other Noggin-like ligands identified in this study may functionally substitute for trunk in terminal patterning. Using *in situ* hybridization and RT-PCR we demonstrate these three ligands are all expressed in the oviparous (sexual) ovary during oogenesis (but not the viviparous ovary), and have distinct expression patterns. None of these ligands are maternally provided to the developing oocyte. In the absence of a ligand, and the temporally restricted expression of the receptor *torso*, it is unlikely that the canonical terminal patterning system is affecting embryo patterning.

Consistent with this idea, although dp-ERK activation is seen throughout the viviparous and oviparous oocytes, it clears from the oviparous (sexual) oocyte in an anterior to posterior sequence at the onset of vitellogenesis possibly as a result of yolk deposition from the anterior. Early activation of dp-ERK throughout the viviparous (asexual) oocyte is independent of *Ap-tor*, as no RNA for *Ap-tor* is detected (Supplementary Fig. 4), implicating the involvement of another tyrosine kinase pathway, such as EGF or FGF signaling, in establishing this initial activation of dp-ERK.

In oviparous oocytes, dp-ERK is cleared from the oocyte from the anterior to the posterior. This clearance is initiated before we can detect *Ap-tsl* expression in the posterior follicle cells. But does coincide with the deposition of yolk into the oocyte. A mechanism based on clearance of dp-ERK is inconsistent with the canonical terminal patterning mechanism we see in *Drosophila* and *Tribolium*, where terminal patterning activates dp-ERK (Ghiglione et al., 1999). We also show, based on the morphology of the adjacent follicle cells, dp-ERK is already restricted to the posterior pole of the oocyte prior to *Ap-tsl* RNA being detected in the posterior follicle cells. *Ap-tsl* RNA continues to be expressed by these posterior follicle cells until the oocyte is mature, and long after dp-ERK staining is no longer visible in the oocyte. Thus implying that the restriction of dp-ERK to the posterior follicle cells is independent of *Ap-tsl* expression. Together, these data imply that *tsl* has a function, independent of dp-ERK activation, in the oviparous ovary. Consistent with this idea *Ap-tsl* is also expressed in viviparous ovaries in posterior follicle cells adjacent to the developing embryo after incorporation of the endosymbiotic bacteria and again in the posterior follicle cells as the embryo reaches maturity. We postulate that the timing of *Ap-tsl* expression may be related to maturation of the embryo/oocyte, and not axial patterning. However, functional studies such as maternal RNAi, which are not currently possible in the pea aphid, would be required to confirm this.

Consistent with the view that canonical terminal patterning is not active in either the pea aphid or the honeybee, genes that we know are targets of this pathway in *Tribolium* and *Drosophila*, including *tailless*, *wingless*, and *huckebein* are not expressed in domains consistent with activation by localized dp-ERK, or by localized *torso-like* RNA (Fig. 9). In the honeybee maternal *tailless* RNA becomes localized (Wilson and Dearden, 2009) and *huckebein* is not expressed early in development (Supplementary Fig. 6). *Am-huckebein* RNA is only detected in neuroectoderm relatively late in embryogenesis, similar to *Tribolium* (Kittelmann et al., 2012), suggesting that *huckebein* has come under control of the terminal-patterning pathway in the lineage leading to *Drosophila*.

In the pea aphid neither *tailless* nor *wingless* RNA are detected in blastoderm stage, or early germ band invagination stage, oviparous (sexual) embryos. Yet, in viviparous (asexual) embryos, where there is no early expression of *tsl*, these RNAs are detected in patterns consistent with those seen in other insects (Schoppmeier and Schroder, 2005; Schroder et al., 2000; Wilson and Dearden, 2009).

Despite the absence of canonical terminal patterning in both the honeybee and pea aphid, torso-like orthologs are expressed in the ovaries of bees and aphids, in patterns that imply roles in active oogenesis. Whatever the biological role of torso-like in these cells, its biochemical activity remains the same,

as expressing versions from different species in *Drosophila* gives a similar phenotype. This molecular activity, suggested to be that of a perforin (Kondos et al., 2010; Lukoyanova and Saibil, 2008; Stevens et al., 2003), is conserved between these different species, despite differences in expression patterns. We propose, therefore, that the evolutionary changes in torso-like function are due to *cis*-regulatory evolution causing differences in the temporal and spatial expression of a functionally conserved protein and that these *cis*-regulatory changes have allowed torso-like to become co-opted into terminal patterning in the lineage leading to Diptera and Coleoptera. That the function of this protein can evolve is shown by *Ap-tslr*, which, in *Drosophila* assays, has a new molecular function.

Evolution of the terminal patterning pathway

Torso-like is the most widely conserved component of the canonical terminal-patterning pathway (Table 1). Orthologs are found in all currently sequenced insect genomes, and it likely arose in the pan-crustacean lineage ~500 million years ago. However, the origins and evolution of the ligand and receptor in the *Drosophila* terminal patterning are less easy to resolve. The ligand is derived from an ancient clade of Noggin-like proteins that have, in arthropods, evolved into PTTH and trunk genes. It is unclear when this occurred, as the genome of a chelicerate has a trunk-like gene, whilst all other trunk-like proteins are found in holometabolous insects. This finding implies either convergent evolution of the chelicerate trunk, or, based on the accepted phylogeny of insects (Savard et al., 2006) and arthropods (Regier et al., 2010), five independent losses of trunk in the phylogeny (Fig. 9). This second scenario is supported by the presence of a small conserved domain in the NL and trunk proteins, which is not present in the PTTH proteins (Supplementary Fig. 2). This indicates that trk and PTTH evolved much earlier in the arthropod lineage than has been previously proposed (Grillo et al., 2012).

Recent findings have, however, demonstrated that in *Drosophila*, PTTH and trunk are functionally equivalent (Grillo et al., 2012; Rewitz et al., 2009), implying that these proteins may represent a clade of "trunk/PTTH" proteins rather than separate lineages. We propose that, given the constraints on sequence change imposed by this ligand having to bind and activate the torso receptor, convergent evolution has acted to produce very similar variants of this protein in different species. Co-evolution of the protein and receptor is also suggested by data that shows that the *Bombyx* PTTH protein cannot effectively activate the *Drosophila* torso receptor (Rewitz et al., 2009).

We propose, that the trk/PTTH, tor, MAPK connection is an ancient one, present in the common ancestor of arthropods but with no role in terminal pattering in these species. Here we present data that *Ap-torso* RNA is found in the prothoracic gland of aphids, reflecting the expression seen in the holometabolous insects *Drosophila* and *Bombyx* (Rewitz et al., 2009). This implies that the role of *torso* signaling in the prothoracic gland may be a conserved and ancient function of the trk/PTTH/tor signaling pathway in insects. In insects the prothoracic gland responds to PTTH hormone to produces ecdysteroids and regulate molting (reviewed in Gilbert et al., 2002; Watson and Spaziani, 1985a, b). In Crustacea, ecdysteroids are produced by a specialized structure known as the Y-gland situated near the antennae (Watson and Spaziani, 1985a, b), and in chelicerates the Schneider's gland-Tropfenkomplex, located in the prosoma and abdomen, is the main site of ecdysone biosynthesis (Craig, 2003; Matsumoto et al., 1992). We infer that the trunk-like protein we have identified in *Ixodes* may have a role in regulating ecdysone biosynthesis and molting.

Torso-like evolved in the pan-crustacean lineage, and our data show that torso-like likely has roles in the ovary of the honeybee and pea aphid that are unrelated to a role in modulating torso activity. Torso-like has recently been shown to be expressed in the prothoracic gland of *Drosophila* and mutations in *torso-like* have been shown to cause developmental delays, consistent with a role for *torso-like* in ecdysteroid production (Grillo et al., 2012). Intriguingly, we observe expression of *torso-like* in structures of the adult brain immediately anterior of the prothoracic segment, raising the possibility that *torso-like* is similarly involved in modulating ecdysone production by the prothoracic gland. We have also shown that genes that are ancestrally related to trunk (*Ap-NL1*, *Ap-NL2* and *Ap-PTTH*) are all expressed during brain development or in regions of the mature brain.

We propose that the terminal patterning pathway known in *Tribolium* and *Drosophila* represents the capture of an ancient signaling mechanism involved in neuroendocrine signaling into a novel role providing terminal patterning information during early embryogenesis. Recruitment of this pathway has facilitated the co-option of target genes, like *tailless*, *huckebein* and *wingless* into control by this pathway. This hypothesis is supported by the expression of these target genes in other insects. In the honeybee,

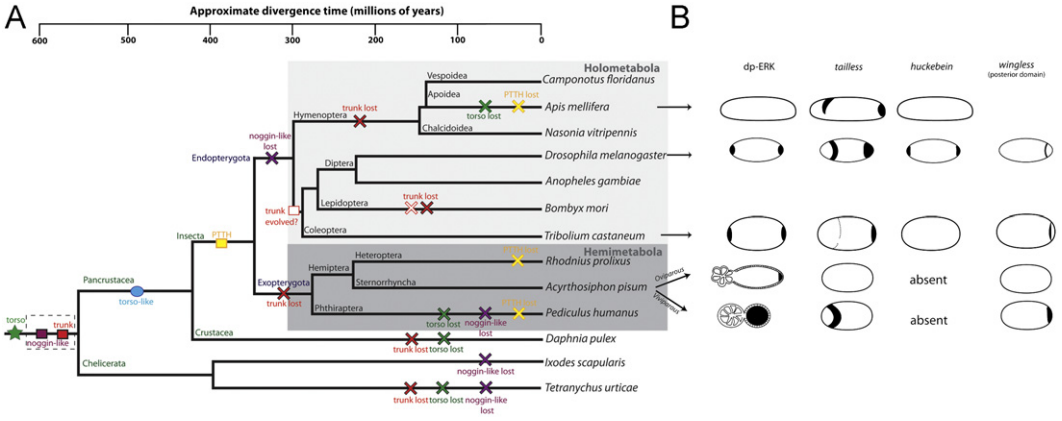

Fig. 9. Model for the evolution of the canonical terminal patterning components: (A) accepted phylogeny of insects modified from Dearden et al. (2010) and incorporating the divergence of insects and chelicerates which is estimated to have occurred 550 million years ago (Regier et al., 2010). The lineages leading to Trombidiforms (*Tetranychus urticae*) from the Paristiforms (*Ixodes scapularis*) diverged ~400 million years ago (Jeyaprakash and Hoy, 2009). Components of the terminal patterning pathway, and associated molecules, were mapped onto the arthropod phylogeny based on the phylogenetic data in Fig. 1. (B) Cartoons demonstrating expression domains (Kittelmann et al., 2012; Schoppmeier and Schroder, 2005; Schroder et al., 2000; Wilson and Dearden, 2009) of genes targeted by the canonical terminal patterning pathway. This model implies that that the posterior cap of *wingless* RNA and anterior stripe of *tailless* RNA were present in the ancestor of insects, but that these domains were historically established in the absence of canonical terminal patterning.

Table 1
Presence/absence of components of the canonical patterning system in the genomes of other insects and non-insect arthropods.

Species[b]	Trunk	Torso	Torso-like	Embryonic expression of targets of the canonical terminal system[a]			
				Dp-ERK	Tailless	Huckebein	Wingless
D. melanogaster	✓	✓	✓	✓	✓	✓	✓
A. gambiae	✓	✓	✓	✓	?		
B. mori	X	✓	✓				
T. castaneum	✓	✓	✓	✓	✓	X	✓
N. vitripennis	X	✓	✓	X	X		
A. mellifera	X	X	✓	X	X	X	
C. floridanus	X	✓	✓				
P. humanus	X	X	✓				
A. pisum	X	✓	✓(×2)	X	X	Absent	X
R. prolixus	X	✓	✓				
D. pulex	X	X	✓				
I. scapularis	✓	✓	X				
T. urticae	X	X	X				

[a] Refers to expression being under control of the canonical terminal-patterning system rather than presence or absence of these genes in the genome.
[b] *References*: *D. melanogaster* (Bronner and Jackle, 1991; Casali and Casanova, 2001; Casanova, 1990; Casanova et al., 1995; Jimenez et al., 2000; Savant-Bhonsale and Montell, 1993; Sprenger et al., 1989). *Anopheles gambiae* (Goltsev et al., 2004), *B. mori* (Dearden et al., 2006). *T. castaneum* (Grillo et al., 2012; Schoppmeier and Schroder, 2005; Schroder et al., 2000). *N. vitripennis* (Lynch et al., 2012; Lynch et al., 2006). *A. mellifera* (Dearden et al., 2006; Wilson and Dearden, 2009), *A. pisum* (Shigenobu et al., 2010). All other data points were derived from this study.

tll RNA is maternally provided and RNA is localized during early embryogenesis to the posterior of the developing embryo, the anterior expression domain is regulated by *otd1* (Wilson and Dearden, 2009). In the hymenopteran *N. vitripennis*, which possesses orthologs of both PTTH and tor, both the anterior and posterior expression domains of *tll* are dependent on *otd1* (Lynch et al., 2006). The molecular mechanism that establishes the conserved anterior domain of *tll* expression is evolutionarily labile, as *otd* is not expressed early in viviparous aphid development and cannot be regulating *Ap-tll* expression (Duncan et al., in press; Huang et al., 2010). The anterior domain of *tll* has been suggested to be less important than the posterior domain for axial patterning (Lynch et al., 2006; Schroder et al., 2000), but the posterior expression domain of *tll* appears to be restricted to the holometabolous insects. *Wingless* is expressed in the posterior of the embryo or the posterior growth zone during embryogenesis in insects (Dearden and Akam, 2001; Nagy and Carroll, 1994), crustaceans (Nulsen and Nagy, 1999) and non-insect arthropods (Damen, 2002). This expression pattern is ancient, and pre-dates the evolution of *torso-like* and canonical terminal patterning. Taken together these data imply that the genes downstream of terminal patterning in *Drosophila* have ancestrally been expressed in anterior and/or posterior domains in the absence of the canonical patterning pathway, and that it is the capture of regulation of these genes that has allowed an ancestral system to be co-opted into patterning the terminal regions of the holometabolous insects, *Drosophila melanogaster* and *Tribolium castaneum*.

Acknowledgments

This project was funded by a Gravida grant to P.K.D. (MP04), a University of Otago Research Grant to P.K.D. and a Royal Society of New Zealand Marsden grant to E.J.D. (11-UOO-124). We thank Tahlia Whiting and Meaghan O'Neill for general technical assistance. The authors also wish to thank Gabrielle Drayton and David Teulon from Plant and Food Research for providing us with the pea aphid cultures. We would like to thank Dr. Gregory Davis for sharing his protocol for *in situ* hybridization of dissected germ bands and for critical reading of this manuscript. The authors would also like to thank Dr. Sarah Morgan, Dr. Andrew Cridge and Abigail Romeril for careful reading of the manuscript.

Appendix. Supporting information

Supplementary data associated with this article can be found in the online version at http://dx.doi.org/10.1016/j.ydbio.2013.02.010.

References

Altschul, S.F., Gish, W., Miller, W., Myers, E.W., Lipman, D.J., 1990. Basic local alignment search tool. J. Mol. Biol. 215, 403–410.
Braendle, C., Miura, T., Bickel, R., Shingleton, A.W., Kambhampati, S., Stern, D.L., 2003. Developmental origin and evolution of bacteriocytes in the aphid-*Buchnera symbiosis*. PLoS Biol. 1, E21.
Campos-Ortega, J.A., Hartenstein, V., 1997. The Embryonic Development of *Drosophila melanogaster*. Springer, Berlin.
Casali, A., Casanova, J., 2001. The spatial control of Torso RTK activation: a C-terminal fragment of the Trunk protein acts as a signal for Torso receptor in the *Drosophila* embryo. Development 128, 1709–1715.
Casanova, J., 1990. Pattern formation under the control of the terminal system in the *Drosophila* embryo. Development 110, 621–628.
Casanova, J., Furriols, M., McCormick, C.A., Struhl, G., 1995. Similarities between trunk and spatzle, putative extracellular ligands specifying body pattern in *Drosophila*. Genes Dev. 9, 2539–2544.
Chang, C.C., Huang, T.Y., Cook, C.E., Lin, G.W., Shih, C.L., Chen, R.P., 2009. Developmental expression of *Apnanos* during oogenesis and embryogenesis in the parthenogenetic pea aphid *Acyrthosiphon pisum*. Int. J. Dev. Biol. 53, 169–176.
Chang, C.C., Lee, W.C., Cook, C.E., Lin, G.W., Chang, T., 2006. Germ-plasm specification and germline development in the parthenogenetic pea aphid *Acyrthosiphon pisum*: Vasa and Nanos as markers. Int. J. Dev. Biol. 50, 413–421.
Chang, C.C., Lin, G.W., Cook, C.E., Horng, S.B., Lee, H.J., Huang, T.Y., 2007. Apvasa marks germ-cell migration in the parthenogenetic pea aphid *Acyrthosiphon pisum* (Hemiptera: Aphidoidea). Dev. Genes Evol. 217, 275–287.
Craig, C.L., 2003. Spiderwebs and Silk: Tracing Evolution from Molecules to Genes to Phenotypes. Oxford University Press, New York; Oxford.
Damen, W.G., 2002. Parasegmental organization of the spider embryo implies that the parasegment is an evolutionary conserved entity in arthropod embryogenesis. Development 129, 1239–1250.
Davis, G.K., Patel, N.H., 2002. Short, long, and beyond: molecular and embryological approaches to insect segmentation. Annu. Rev. Entomol. 47, 669–699.
Dearden, P.K., Akam, M., 2001. Early embryo patterning in the grasshopper, *Schistocerca gregaria:* wingless, decapentaplegic and caudal expression. Development 128, 3435–3444.
Dearden, P.K., Duncan, E.J., Wilson, M.J., 2010. The honeybee: *Apis mellifera*. In: Patel, N.H. (Ed.), Emerging Model Organisms. Cold Spring Harbor Laboratory Press.
Dearden, P.K., Wilson, M.J., Sablan, L., Osborne, P.W., Havler, M., McNaughton, E., Kimura, K., Milshina, N.V., Hasselmann, M., Gempe, T., Schioett, M., Brown, S.J., Elsik, C.G., Holland, P.W., Kadowaki, T., Beye, M., 2006. Patterns of conservation and change in honey bee developmental genes. Genome Res. 16, 1376–1384.
Duncan, E.J., Dearden, P.K., 2010. Evolution of a genomic regulatory domain: the role of gene co-option and gene duplication in the enhancer of split complex. Genome Res. 20, 917–928.

Duncan, E.J., Leask, M.P., Dearden, P.K. The pea aphid (Acyrthosiphon pisum) genome encodes two divergent early developmental programs. Dev Biol., http://dx.doi.org/10.1016/jj.ydbio.2013.01.036, in press.
DuPraw, E.J., 1967. The Honeybee Embryo. In: Wilt, F.H., Wessells, N.K. (Eds.), Methods in Developmental Biology. Thomas Y Cromwell Company, New York, pp. 183–217.
Eddy, S.R., 1998. Profile hidden Markov models. Bioinformatics 14, 755–763.
Furriols, M., Casanova, J., 2003. In and out of Torso RTK signalling. EMBO J. 22, 1947–1952.
Gabay, L., Seger, R., Shilo, B.Z., 1997. MAP kinase *in situ* activation atlas during *Drosophila* embryogenesis. Development 124, 3535–3541.
Garcia-Solache, M., Jaeger, J., Akam, M., 2010. A systematic analysis of the gap gene system in the moth midge *Clogmia albipunctata*. Dev. Biol. 344, 306–318.
Ghiglione, C., Perrimon, N., Perkins, L.A., 1999. Quantitative variations in the level of MAPK activity control patterning of the embryonic termini in *Drosophila*. Dev. Biol. 205, 181–193.
Gilbert, L.I., Rybczynski, R., Warren, J.T., 2002. Control and biochemical nature of the ecdysteroidogenic pathway. Annu. Rev. Entomol. 47, 883–916.
Goltsev, Y., Hsiong, W., Lanzaro, G., Levine, M., 2004. Different combinations of gap repressors for common stripes in *Anopheles* and *Drosophila* embryos. Dev. Biol. 275, 435–446.
Grillo, M., Furriols, M., de Miguel, C., Franch-Marro, X., Casanova, J., 2012. Conserved and divergent elements in Torso RTK activation in *Drosophila* development. Sci. Rep. 2, 762.
Grimm, O., Zini, V.S., Kim, Y., Casanova, J., Shvartsman, S.Y., Wieschaus, E., 2012. Torso RTK controls Capicua degradation by changing its subcellular localization. Development 139, 3962–3968.
Howe, K., Bateman, A., Durbin, R., 2002. QuickTree: building huge Neighbour-Joining trees of protein sequences. Bioinformatics 18, 1546–1547.
Huang, T.Y., Cook, C.E., Davis, G.K., Shigenobu, S., Chen, R.P., Chang, C.C., 2010. Anterior development in the parthenogenetic and viviparous form of the pea aphid, *Acyrthosiphon pisum*: hunchback and orthodenticle expression. Insect Mol. Biol. 19 (2), 75–85.
Jeyaprakash, A., Hoy, M.A., 2009. First divergence time estimate of spiders, scorpions, mites and ticks (subphylum: Chelicerata) inferred from mitochondrial phylogeny. Exp. Appl. Acarol. 47, 1–18.
Jones, D.T., Taylor, W.R., Thornton, J.M., 1992. The rapid generation of mutation data matrices from protein sequences. Comput. Appl. Biosci.: CABIOS 8, 275–282.
Kittelmann, S., Ulrich, J., Posnien, N., Bucher, G., 2012. Changes in anterior head patterning underlie the evolution of long germ embryogenesis. Dev. Biol. 374, 174–184.
Klingler, M., Erdelyi, M., Szabad, J., Nusslein-Volhard, C., 1988. Function of torso in determining the terminal anlagen of the *Drosophila* embryo. Nature 335, 275–277.
Kondos, S.C., Hatfaludi, T., Voskoboinik, I., Trapani, J.A., Law, R.H., Whisstock, J.C., Dunstone, M.A., 2010. The structure and function of mammalian membrane-attack complex/perforin-like proteins. Tissue Antigens 76, 341–351.
Krauss, V., Thummler, C., Georgi, F., Lehmann, J., Stadler, P.F., Eisenhardt, C., 2008. Near intron positions are reliable phylogenetic markers: an application to holometabolous insects. Mol. Biol. Evol. 25, 821–830.
Le Trionnaire, G., Hardie, J., Jaubert-Possamai, S., Simon, J.C., Tagu, D., 2008. Shifting from clonal to sexual reproduction in aphids: physiological and developmental aspects. Biol. Cell/under the auspices of the European Cell Biology Organization 100, 441–451.
Lemke, S., Busch, S.E., Antonopoulos, D.A., Meyer, F., Domanus, M.H., Schmidt-Ott, U., 2010. Maternal activation of gap genes in the hover fly *Episyrphus*. Development 137, 1709–1719.
Lukoyanova, N., Saibil, H.R., 2008. Friend or foe: the same fold for attack and defense. Trends Immunol. 29, 51–53.
Lynch, J.A., El-Sherif, E., Brown, S.J., 2012. Comparisons of the embryonic development of Drosophila, Nasonia, and Tribolium. Wiley Interdiscip. Rev.: Dev. Biol. 1, 16–39.
Lynch, J.A., Olesnicky, E.C., Desplan, C., 2006. Regulation and function of tailless in the long germ wasp *Nasonia vitripennis*. Dev. Genes Evol. 216, 493–498.
Lynch, J.A., Peel, A.D., Drechsler, A., Averof, M., Roth, S., 2010. EGF signaling and the origin of axial polarity among the insects. Curr. Biol. 20, 1042–1047.
Martin, J.R., Raibaud, A., Ollo, R., 1994. Terminal pattern elements in *Drosophila* embryo induced by the torso-like protein. Nature 367, 741–745.
Matsumoto, A., Ishii, S., Kobayashi, H., 1992. Atlas of Endocrine Organs: Vertebrates and Invertebrates. Springer-Verlag, Berlin; London.
Miura, T., Braendle, C., Shingleton, A., Sisk, G., Kambhampati, S., Stern, D.L., 2003. A comparison of parthenogenetic and sexual embryogenesis of the pea aphid *Acyrthosiphon pisum* (Hemiptera: Aphidoidea). J. Exp. Zool. B Mol. Dev. Evol. 295, 59–81.
Mushegian, A.R., Koonin, E.V., 1996. Sequence analysis of eukaryotic developmental proteins: ancient and novel domains. Genetics 144, 817–828.
Nagy, L.M., Carroll, S., 1994. Conservation of wingless patterning functions in the short-germ embryos of *Tribolium castaneum*. Nature 367, 460–463.
Nulsen, C., Nagy, L.M., 1999. The role of wingless in the development of multibranched crustacean limbs. Dev. Genes Evol. 209, 340–348.
Osborne, P., Dearden, P.K., 2005. Non-radioactive *in-situ* hybridisation to honeybee embryos and ovaries. Apidologie 36, 113–118.
Patel, N.H., 1994. Imaging Neuronal subsets and other cell types in whole-mount Drosophila embryos and larvae using Antibody probes. In: Goldstein, L.S.B., Fyrberg, E.A. (Eds.), Drosophila melanogaster: Practical uses in Cell and Molecular biology., 44 ed. Academic Press, London, pp. 446–485.
Patel, N.H., Condron, B.G., Zinn, K., 1994. Pair-rule expression patterns of even-skipped are found in both short and long germ beetles. Nature 367, 429–434.
Rafiqi, A.M., Lemke, S., Schmidt-Ott, U., 2010. Postgastrular *zen* expression is required to develop distinct amniotic and serosal epithelia in the scuttle fly *Megaselia*. Dev. Biol. 341, 282–290.
Regier, J.C., Shultz, J.W., Zwick, A., Hussey, A., Ball, B., Wetzer, R., Martin, J.W., Cunningham, C.W., 2010. Arthropod relationships revealed by phylogenomic analysis of nuclear protein-coding sequences. Nature 463, 1079–1083.
Rewitz, K.F., Yamanaka, N., Gilbert, L.I., O'Connor, M.B., 2009. The insect neuropeptide PTTH activates receptor tyrosine kinase torso to initiate metamorphosis. Science 326, 1403–1405.
Ronquist, F., Huelsenbeck, J.P., 2003. MrBayes 3: Bayesian phylogenetic inference under mixed models. Bioinformatics 19, 1572–1574.
Rorth, P., 1998. Gal4 in the *Drosophila* female germline. Mech. Dev. 78, 113–118.
Rousso, T., Lynch, J., Yogev, S., Roth, S., Schejter, E.D., Shilo, B.Z., 2010. Generation of distinct signaling modes via diversification of the Egfr ligand-processing cassette. Development 137, 3427–3437.
Rubin, G.M., Spradling, A.C., 1982. Genetic transformation of *Drosophila* with transposable element vectors. Science 218, 348–353.
Savant-Bhonsale, S., Montell, D.J., 1993. *torso-like* encodes the localized determinant of *Drosophila* terminal pattern formation. Genes Dev. 7, 2548–2555.
Savard, J., Tautz, D., Richards, S., Weinstock, G.M., Gibbs, R.A., Werren, J.H., Tettelin, H., Lercher, M.J., 2006. Phylogenomic analysis reveals bees and wasps (Hymenoptera) at the base of the radiation of Holometabolous insects. Genome Res. 16, 1334–1338.
Schoppmeier, M., Schroder, R., 2005. Maternal torso signaling controls body axis elongation in a short germ insect. Curr. Biol. 15, 2131–2136.
Schroder, R., Eckert, C., Wolff, C., Tautz, D., 2000. Conserved and divergent aspects of terminal patterning in the beetle *Tribolium castaneum*. Proc. Natl. Acad. Sci. USA 97, 6591–6596.
Shigenobu, S., Bickel, R.D., Brisson, J.A., Butts, T., Chang, C.C., Christiaens, O., Davis, G.K., Duncan, E.J., Ferrier, D.E., Iga, M., Janssen, R., Lin, G.W., Lu, H.L., McGregor, A.P., Miura, T., Smagghe, G., Smith, J.M., van der Zee, M., Velarde, R.A., Wilson, M.J., Dearden, P.K., Stern, D.L., 2010. Comprehensive survey of developmental genes in the pea aphid, *Acyrthosiphon pisum*: frequent lineage-specific duplications and losses of developmental genes. Insect Mol. Biol. 19 (2), 47–62.
Sievers, F., Wilm, A., Dineen, D., Gibson, T.J., Karplus, K., Li, W., Lopez, R., McWilliam, H., Remmert, M., Soding, J., Thompson, J.D., Higgins, D.G., 2011. Fast, scalable generation of high-quality protein multiple sequence alignments using Clustal Omega. Mol. Syst. Biol. 7, 539.
Sprenger, F., Stevens, L.M., Nusslein-Volhard, C., 1989. The *Drosophila* gene *torso* encodes a putative receptor tyrosine kinase. Nature 338, 478–483.
Stern, D.L., Sucena, E., 2000. Preparation of Larval and Adult Cuticles for Light Microscopy. In: Sullivan, W., Ashburner, M., Hawley, R.S. (Eds.), Drosophila protocols. Cold Spring Harbour Laboratory Press, New York.
Stevens, L.M., Beuchle, D., Jurcsak, J., Tong, X., Stein, D., 2003. The *Drosophila* embryonic patterning determinant torsolike is a component of the eggshell. Curr. Biol. 13, 1058–1063.
Tautz, D., Pfeifle, C., 1989. A non-radioactive *in situ* hybridization method for the localization of specific RNAs in *Drosophila* embryos reveals translational control of the segmentation gene hunchback. Chromosoma 98, 81–85.
Thompson, J.D., Higgins, D.G., Gibson, T.J., 1994. Clustal-W—improving the sensitivity of progressive multiple sequence alignment through sequence weighting, position-specific gap penalties and weight matrix choice. Nucleic Acids Res. 22, 4673–4680.
Watson, R.D., Spaziani, E., 1985a. Biosynthesis of ecdysteroids from cholesterol by crab Y-organs, and eyestalk suppression of cholesterol uptake and secretory activity, *in vitro*. Gen. Comp. Endocrinol. 59, 140–148.
Watson, R.D., Spaziani, E., 1985b. Effects of eyestalk removal on cholesterol uptake and ecdysone secretion by crab (*Cancer antennarius*) Y-organs *in vitro*. Gen. Comp. Endocrinol. 57, 360–370.
Whelan, S., Goldman, N., 2001. A general empirical model of protein evolution derived from multiple protein families using a maximum-likelihood approach. Mol. Biol. Evol. 18, 691–699.
Wilk, R., Weizman, I., Shilo, B.Z., 1996. *trachealess* encodes a bHLH-PAS protein that is an inducer of tracheal cell fates in *Drosophila*. Genes Dev. 10, 93–102.
Wilson, M.J., Abbott, H., Dearden, P.K., 2011. The evolution of oocyte patterning in insects: multiple cell-signaling pathways are active during honeybee oogenesis and are likely to play a role in axis patterning. Evol. Dev. 13, 127–137.
Wilson, M.J., Dearden, P.K., 2009. *Tailless* patterning functions are conserved in the honeybee even in the absence of Torso signaling. Dev. Biol. 335, 276–287.
Zdobnov, E.M., Bork, P., 2007. Quantification of insect genome divergence. Trends Genet. 23, 16–20.